Francisco Miranda Sacarrão

Licenciado em Ciências da Engenharia Biomédica

Produção de estruturas 3D porosas à base de polímeros piezoelétricos para aplicação em engenharia de tecidos

Dissertação para obtenção do Grau de Mestre em
Engenharia Biomédica

Orientador: Maria do Carmo Henriques Lança, Professor Auxiliar, Faculdade de Ciências e Tecnologias da Universidade Nova de Lisboa

Co-orientador: Jorge Alexandre Monteiro Carvalho Silva, Professor Auxiliar, Faculdade de Ciências e Tecnologias da Universidade Nova de Lisboa

FACULDADE DE CIÊNCIAS E TECNOLOGIA
UNIVERSIDADE NOVA DE LISBOA

November, 2018

Science is a way of thinking much more than it is a body of knowledge
Carl Sagan

Acknowledgments

Writing a master thesis requires a lot of work and dedication, but also a lot of help, support and orientation throughout and I would like to take time to express my sincere acknowledgements to all the people that have helped me to get this far.

Firstly, I would like to thank Professor Carmo Lança for the opportunity to work and learn with her. Thank you so much for all the guidance and positive ideas during these months.
I also would like to thank my co-advisor, Professor Jorge Silva, for all his help and guidance in the lab, especially in the end of this master thesis.

I would like to thank to Professor João Borges and Professor Ana Aguiar for all the aid and support during this work. Also, to all the investigators in the lab, for taking their time to teaching me new techniques and how to work with different equipment. Especially Clarinda Costa, Raquel Viveiros and Teresa Casimiro for all their help.

To my big friends Hudson Neto and Pedro Pinto, for all their support and distractions in times of need.

To my friends Tiago Ferreira, Guilherme Oliveira, Nuno Ferreira, João Papel, Joaquim Vitorino and João Teixeira for all moral support.

To my girlfriend, Beatriz Valpradinhos, for listening even though she didn't understand half of the things I said and for never letting me give up when my spirit was down.

A special thanks to my family, more especially my parents, for all the support and for putting up with me in times of stress. Without you I would never, ever, come this far. I'll always be grateful for all your love and support, and for having you in my life.

Abstract

Biomaterial scaffolds are designed to mimic the extracellular matrix and will act as a physical support to promote the regrowth of the tissue and the migration of proteins. This field is still in development because of the emerging need of transplants and its biocompatibility issues.

Polyvinylidene fluoride (PVDF) is a fluoropolymer and biopolymer. PVDF membranes have already been produced and evaluated as scaffolds. However, these membranes did not make use of the β-phase of PVDF, that exhibits piezoelectric properties. Because of the role played by piezoelectric response on bone remodelling, piezoelectric scaffolds can be exploited to enhance the efficacy of repair in the bone tissue.

In this work PVDF membranes were produced by solvent-casting and particulate leaching and CO_2 supercritical methods in order to get a membrane with interconnected porosity.

Optimised PVDF membranes by CO_2 supercritical were obtained but not by other method. The membranes showed the presence of β-phase. DRX and SEM images displayed a highly interconnected porous structure. The porosity of the structure, cell adhesion, biocompatibility, electrical polarization and bioactivity were also studied in this work.

Keywords: biomaterial, PVDF, piezoelectric properties, β-phase, cell adhesion

Resumo

Os biomateriais são projetados para reproduzir a matriz extracelular e atuam como suporte físico que promove o crescimento do tecido e a migração das proteínas. Esta área está em desenvolvimento devido à crescente necessidade de transplantes e problemas relacionados com a biocompatibilidade.

O Fluoreto de polivinilideno (PVDF) é um fluoropolímero e um biopolímero. As membranas de PVDF foram produzidas e avaliadas como membranas para as células. No entanto, estas membranas não fizeram proveito da fase β do PVDF, que exibe propriedades piezoeléctricas. Devido ao papel que a resposta piezoeléctrica na remodelação do osso, as membranas piezoeléctricas podem ser aproveitadas para aumentar a eficácia de reparação do tecido ósseo.

Neste trabalho foram produzidas membranas de PVDF pelos métodos de *solvent-casting and particulate leaching* e CO_2 supercrítico de forma a se obter uma membrana com poros interconectados.

As membranas otimizadas de PVDF foram obtidas apenas pelo método do CO_2 supercrítico e não por outro tipo de método. As membranas produzidas puderam confirmar a presença de fase β. As imagens obtidas por DRX e SEM evidenciaram uma estrutura interconectada altamente porosa. A porosidade da estrutura, os testes de adesão celular, a polarização elétrica e os ensaios de bioactividade também foram estudados.

Keywords: biomaterial, PVDF, propriedades piezoeléctricas, fase β, adesão celular.

List of abbreviations

3D	Three Dimensional
DAPI	4′,6-diamidino-2-phenylindole
DMF	N, N-Dimethylformamide
DMSO	Dimethyl Sulfoxide
DSC	Differential Scanning Calorimetry
EDS	Energy-Dispersive X-Ray Spectroscopy
FBS	Fetal Bovine Serum
FIB-SEM	Focus Ion Beam Scanning Electron Microscope
FTIR	Fourier-Transform Infra-Red Spectroscopy
PBS	Phosphate Buffered Saline
PVA	Polyvinyl Alcohol
PVDF	Polyvinylidene Fluoride
PVDF-TrFE	Polyvinylidene Fluoride-Trifluoroethylene
SBF	Simulated Body Fluid
SEM	Scanning Electron Microscope
TSDC	Thermally Stimulated Discharge Current
UNOS	United Network for Organ Sharing
XRD	X-Ray Diffraction

List of symbols

M_w	Molecular Weight
σ	Mechanical Stress
V	Voltage
D	Dielectric Displacement
E	Electric Field
d	piezoelectric charge constant

Table of contents

List of Figures

1

Motivation and Objectives

Over the recent years, tissue engineering has been gaining an increasingly important role in our society. This field brings together knowledge from different areas, among which stand out clinical medicine, engineering and science. Tissue engineering is defined by Viola et al. [1] as "*the application of principles and methods of engineering and life sciences toward fundamental understanding of structure-function relationships in normal and pathological mammalian tissues and the development of biological substitutes to restore, maintain, or improve tissue function*".

Many biological materials possess piezoelectric properties. Human tissues like bone and tendons, collagen, nucleic acids, myosin and actin display this property [2]. Recent studies have proved that electric stimulation improved cell adhesion and proliferation in those different tissues [3-4].

In this work, the piezoelectric effect as a property of implants is going to be analysed using synthetic piezoelectric polymers like polyvinylidene fluoride (PVDF) and its copolymer. These polymers present a higher piezoelectric coefficient compared to other biological material [5]. Also, they present the characteristics of a biomaterial.

The main objective of this work is the study of the biocompatibility of porous 3D matrices from piezoelectric polymers. Porous scaffolds of PVDF, produced using CO_2 supercritical method, are polarized and then characterized to be tested in vitro to evaluate its biological compatibility.

This work will allow a more in-depth understanding of the use of piezoelectric polymers, such as PVDF, as a biomaterial 3D porous structure and how it can help the promotion of the regrowth and regeneration of damaged cells, regarding their electric properties.

2 Introduction

2.1 Biomaterial

Biomaterial as defined by D. F. Williams [6] is “a material designed to take a form that can direct, through interactions with living systems, the course of any therapeutic or diagnostic procedure”. This field of science is not recent, but the advance of technology has allowed an increase of applications. Most common are joint replacements, bone plates, blood vessel prostheses, heart valves and so many other applications.

The advancement of the study in this field arises from the need to improve the current methods of repair, replacement or regeneration treatment. Before, the most used methods were the transplant of tissue from one place to another of the same patient, also known as autograft, or from one patient to another one, called allograft. These methods have been useful, but they face limitations such as biocompatibility issues, problems guaranteeing tissue for every patient in need and these procedures involve some pain and risk of infection [7]. According to Global Observatory on Donation and Transplantation [8] statistics, there has been an increase of 5.8% of transplanted organs from 2014 to 2015 and according to UNOS [9] more than 7000 people died in 2016 while waiting for an organ transplant. The use of biomaterials’ scaffolds may show a significant improvement on mitigating the lack of transplants.

Biomaterial scaffolds are 3D polymeric materials designed to serve as physical support of cells and mimic extracellular matrix environment in order to promote cell growth and migration of nutrients and proteins [10]. There are many properties to consider when developing a biomaterial. The most important is biocompatibility since the scaffold needs to behave as a biological tissue so the cells can adhere while avoiding interactions that will trigger the immune system’s response. Then there is biodegradability, which is not an obligatory property in all biomaterials, that guarantees the replacement of the implant by the living tissue. Mechanical properties are also relevant in the design of the biomaterial. It is important to guarantee that the implant can mimic the mechanical properties of the tissue that is replacing. It should be able to sustain the same mechanical stresses while having enough void volume to facilitate vascularization and tissue implantation. Finally, there are electrical properties that will be the focus of this work. This property is considered since some devices deliver power or detect electrical signals. In 1985, N. B. Patel et al. [11] presented a study where they concluded that the neurite growth was influenced by the stimulation of electrical current. In the presence of current, it occurred an increase on the growth cone extension. On the contrary, when the current polarity was reversed, it occurred a reduction of the growth.

2.2 Piezoelectrics

The piezoelectric response of the materials depends vastly on the molecular structure and how atoms are arranged in their lattice. The polarization occurs when the average position of the positive ions does not equal the average position of the negative ions. The net polarization is caused due to the alignment of the dipoles in the same direction. This situation happens when the temperature is below the Curie temperature where the energy is low, and the polymer has an asymmetric crystal lattice. If the temperature is above the Curie temperature the molecular structure will have an overlap between both positive and negative ions resulting on a zero-net polarization. In piezoelectric materials, the Curie temperature (*Tc*) is defined as the temperature at which the material loses the ability of sustaining polarization. The polar crystalline phase is possible to obtain through many processes such as mechanical orientation, thermal annealing and high voltage treatment [12].

The electric poling can be done to develop a net polarization below the Curie temperature by applying an electric field. Cells react to the presence of a charged surface [13]. By polarizing the polymer, its surface will be charged because of the orientation of the dipoles. This process can be made with two major techniques: DC poling and corona charge. The first technique, DC poling, is implemented by applying a static electric field at a given temperature for a period of time that will permit the mobile entities to orientate themselves with the field. Poling efficiency is tested using a thermally depolarisation current (TSDC) technique at constant temperature (described in section 3.3). Corona charging consist of applying a high enough electric field to a gas. This causes ionization of the gas and the ions and/or electrons are accelerated and impact on the surface to be charged. This last technique was not tested in this work.

Piezoelectricity is a property present on some materials in which a change in the polarization caused by external applied forces can induce an electric charge [14]. This phenomenon was discovered in 1880 by the brothers Pierre and Jacques Curie. They suggested the possibility of a relationship between mechanical stress and electricity. Later, the same authors published a study proving their theory, having conducted experiments with tourmaline, quartz, topaz, cane sugar and Rochelle salt crystals [15]. In these experiments, the authors realized that the crystals would vibrate at different frequencies when an electromagnetic field is applied.

There are two types of piezoelectric effects: direct piezoelectric effect and inverse piezoelectric effect. The first one, as seen on figure 1, consists on the generation of an electric field whenever the material is subject to mechanical stress, σ [16]. The second one corresponds to the opposite effect, in which occurs the deformation of the material when an electric field is applied to the material.

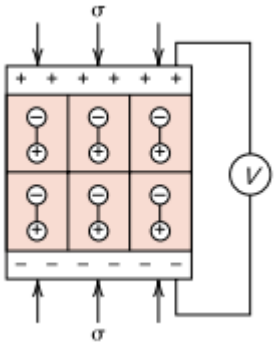

Figure 1- Voltage generated caused by stress compression of the material [14].

The piezoelectricity can be measured combining the effect of the electrical and mechanical work done in the material using the following equations 2.1 and 2.2 where D is the electric charge density displacement, ε is permittivity, σ is mechanical stress, E is electric field, S is strain, s is compliance and d is the piezoelectric charge constant.

$$\{\boldsymbol{D}\} = [\boldsymbol{d}]\{\sigma\} + [\boldsymbol{\varepsilon}^{\sigma}]\{\boldsymbol{E}\} \qquad 2.1$$

$$\{\boldsymbol{S}\} = [\boldsymbol{s}^{\boldsymbol{E}}]\{\sigma\} + [\boldsymbol{d}^{\boldsymbol{t}}]\{\boldsymbol{E}\} \qquad 2.2$$

The piezoelectric charge constant, [d], is a matrix holding the different values of the piezoelectric charge constant, d_{ij} for each tensor indices. The index i denotes the direction of the generated voltage and the index j refers to the direction of the applied stress as shown on figure 2. The axes are numbered from 1 to 3, where 1 is the machine direction, 2 is the perpendicular planar direction and 3 is corresponds to the thickness of the element.

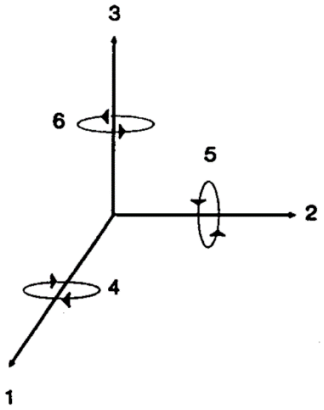

Figure 2 - Piezoelectric axes used to describe the orientation of a crystal. Adapted from [17].

2.3 Bone Tissue

Bone is an organ that is composed by a specialized connective tissue. Within this tissue we can distinguish different types of cells like osteoblasts, osteocytes and osteoclasts [18]. Osteoblasts are cells located in the lacunae of the bone and are responsible for the formation of the bone itself. Once the cells are trapped inside the matrix, they will secrete originating osteocyte cells. Osteocytes are the most abundant cells in the bone and they can act as a mechanosensory cells since they can control the cell-cell interactions with osteoclasts and osteoblasts [19]. At last, the osteoclasts is a type of cell responsible for the breakdown of the bone tissue and in order to begin its repair and remodelling. Also, it is the regulator of the calcium level present in the blood. This is achieved by digesting the proteins and the minerals present in the bone.

The bone possesses distinct functions such as support for the vital organs and the locomotion of the body. It is also a storage of mineral present in the human body, such as calcium and phosphate, and it harbours the bone marrow that is the main site of production of blood cells.

With regard to the constitution of the bone, we can distinguish two different phases that are responsible for different characteristics at the same time like flexibility and toughness. The organic phase is formed mostly by collagen fibers, being the most abundant the collagen fiber type 1 (95%) and some glycoproteins and proteoglycans. This phase confers properties like toughness and resistance to the bone. The inorganic phase, or mineral phase, represents about half of the bone matrix's weight and it is mostly home of minerals like hydroxyapatite (a calcium phosphate) and other minerals in smaller quantities like calcium carbonate [20].

Piezoelectricity on the bone has been studied by Fukada and Yasuda and this effect was observed when the shearing force is applied to collagen fibers [21].

Also, D. Rossi and P. Dario [22] stated that "Bone healing stimulation by electrical charges delivered by piezoelectric polymers implants can potentially play a significant role in therapy of nonunion-fractures".

2.4 Polyvinylidene fluoride

PVDF is a semi crystalline fluoropolymer that can exhibit piezoelectric activity and it is formed by the polymerization of vinylidene. This property comes from the fact that in some phases, the fluorine and hydrogen atoms are placed in the opposite sides of the carbon backbone, generating

a strong dipole [23]. Besides that, it is having a huge role on the production of biomaterials due to the fact that fluoropolymers are biocompatible and chemical inert [24].

The piezoelectric properties of PVDF was discovered in 1969 by H. Kawai [25] and exists in four different crystalline phases which are α, β, γ and δ. Each one of these has a different conformation, but α-phase is the only one that does not possess piezoelectric properties because its conformation consists of trans-gauche-trans-gauche resulting on zero net dipole moment. Despite that, α-phase is the most common phase for PVDF and can be obtained by crystallization by either fusion or cooling of the material. The calculated density of α-phase is 1,92 g/cm^3 and its melting temperature it is 170 °C [26].

The β-phase has an all-trans conformation and between the others, is the one that exhibits the highest dipolar moment being the phase used to exploit piezoelectric properties as it is shown on figure 3. These phases can suffer conversion from one to another by changing properties such as temperature or the electrical field. β-phase can be obtained from α-phase by stretching six times at 90 °C [27]. The calculated density for β-phase is 1,97 g/cm^3 and the melting temperature varies from 168 °C to 191 °C being this variation due to the different methods of preparation [28].

Both α and β-phases are highly used in biomedical applications despite having different objectives since α-phase supports higher cell metabolic activity than β-phase. The latter is used as an artificial membrane with piezoelectric properties to enhance and promote regrowth damaged cells.

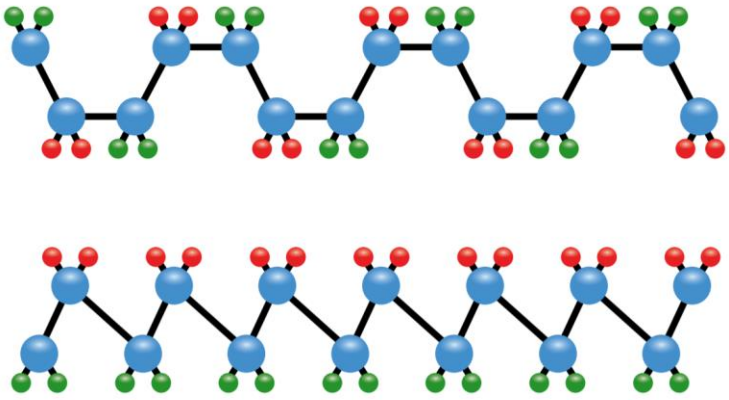

Figure 3 - Schematic representation α (upper image) and β (bottom image) conformations. Blue, red and green are Carbon, Fluor and Hydrogen, respectively. Adapted from [29].

Besides PVDF, there is its copolymer polyvinylidene fluoride-tetrafluoroethylene (PVDF-TrFE) that only exhibits β-phase due to its own natural conformation and has a higher piezoelectric

response when compared to PVDF alone [30]. An example of those values is represented on table 1 showing different piezoelectric coefficients for β-phase PVDF.

Table 1 - *Piezoelectric charge constants for different modes of PVDF* [30].

Piezoelectric Strain (pC/N)	$d_{31} = 21$	$d_{32} = 2.3$	$d_{33} = -26$	$d_{24} = -27$	$d_{15} = -23$

2.5 PVDF studies applied to biomedical field

The discovery of this property of PVDF opened doors to new opportunities of research with importance on biomedical devices.

The electric current proved worthy of facilitating the process of treatment and repair of damaged living tissue. E. Fine et al. [31] performed a research on rats to analyze the efficiency of the PVDF copolymer, PDVF-TrFE, as an implant used to promote nerve regeneration. This research was accomplished using polarized tubes of PVDF-TrFE to act as nerve guidance channels. This study showed remarkable results since nerves regenerated in poled tubes with the piezoelectric copolymer had a superior number of myelinated axons when compared to tubes that contained no piezoelectric activity, as is shown on figure 4. Besides this, there was a difference in the number of myelinated axons as it is seen on figure 5. The number of myelinated axons regenerated was higher when using positive poled PVDF-TrFE copolymer but when it is negative poled it is still higher than the control samples where there was no polarization displayed.

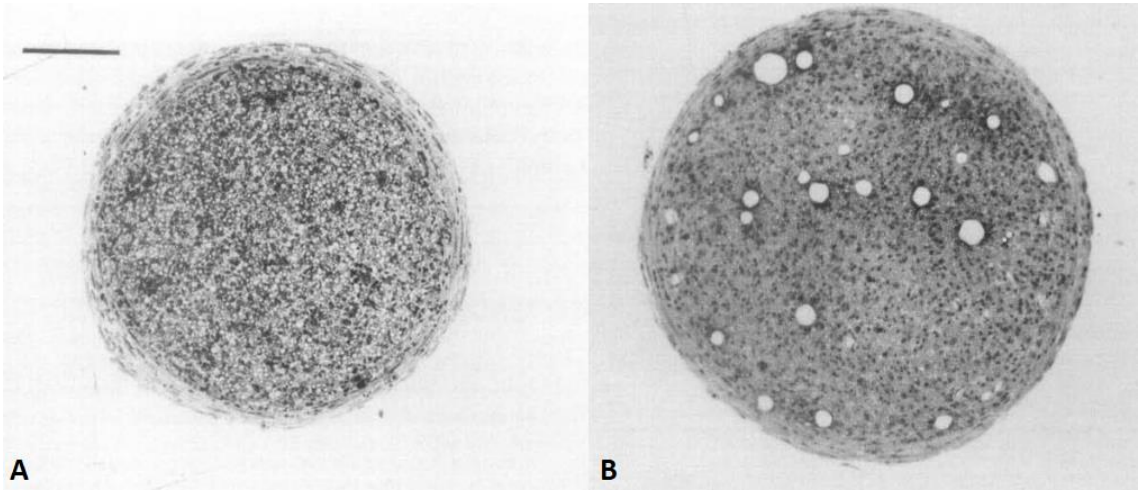

Figure 4 - Transverse section at midpoint of nerve cables regenerated through PVDF-TrFE copolymer. (A) Low power micrograph of nerves regenerated in unpoled tubes. (B) Low power micrograph of nerves regenerated in poled tubes. Adapted from [30].

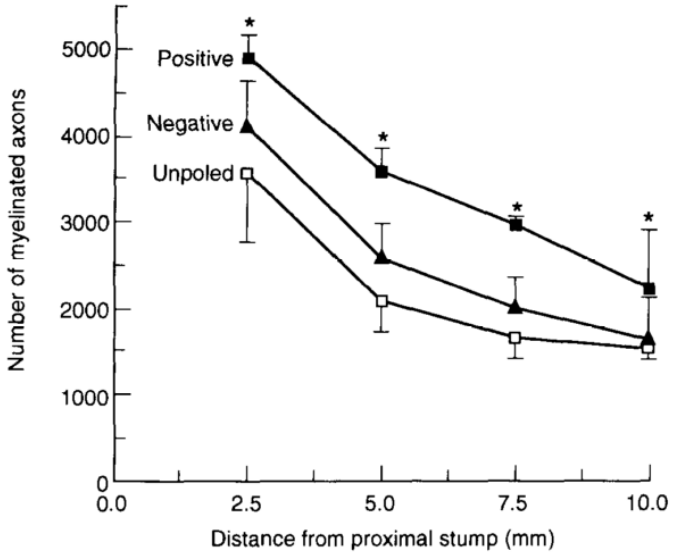

Figure 5 - Relationship between the number of myelinated axons and the distance from proximal stump in positive, negative and unpoled PVDF-TrFE. Adapted from [30].

This study acknowledged the piezoelectric properties of the PVDF-TrFE copolymer as a material capable of favouring the regeneration of nerve and enabling the repair of damaged tissue.

The research done on this polymer has been expanding since its discovery and different applications have been developed using tubes and film [16]. The main objective of this work is the development of 3D porous membranes and the work done on this field is quite recent. In 2015, J.

Nunes-Pereira et al. [32] performed a research with the aim of studying porous membranes of PVDF and its copolymer PVDF-TrFE and their mechanical and piezoelectric properties for tissue engineering. The method of production involved was the solvent casting technique. Then the membranes were characterized in order to determine the porosity and pore size. The results were noticeable showing in figure 6 the comparison of the porosity and the average pore size between PVDF and its copolymer. It was also evaluated the phases present to confirm the presence of β-phase using FTIR and the degree of crystallinity of the polymer.

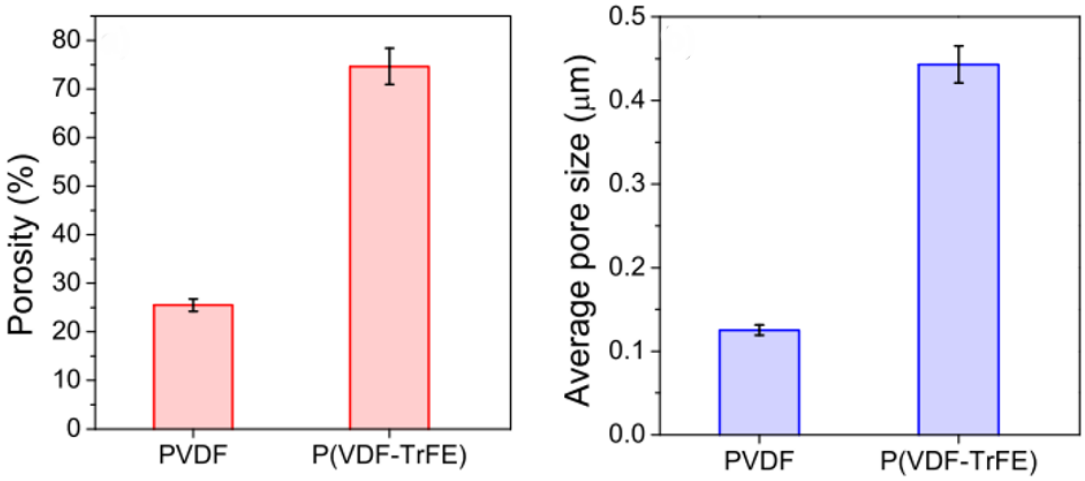

Figure 6 - Degree of porosity and average pore size of the polymer and copolymer membranes. Adapted from [32].

This work brought interesting conclusions regarding the interaction with the living tissue. Cell proliferation was verified with both polymers, but it was demonstrated that higher pore size and lowest degree of porosity were important for getting better results. This contribution has provided a major breakthrough in how scaffolds can be used as biomedical implants because the control of either pore size or degree of porosity can induce the pretended response of cellular regeneration of a specific tissue. The copolymer PVDF-TrFE presents higher pore size and degree of porosity than the PVDF itself showing the best characteristics to be used in a medical implant.

Since there are already many studies about properties and the relationship between the scaffolds and the living tissue, the new challenge is the development of 3D porous membranes of PVDF. In 2016, D. M. Correia et al. [33] developed different strategies to answer this challenge that consisted on three methods: solvent-casting particulate leaching, solvent casting with a 3D nylon template and freeze extraction with a 3D PVA template. Of the three mentioned by the authors, the first is the one that presents bigger porous size. These porous will have a size on the same range of the salt used as a porogen. It is also stated by D. M. Correia et al. [33] that NaCl was the salt used as

a porogen that present the highest porosity and promotes an increase of the sample crystallinity until a certain concentration. When the concentration of salt surpasses a critical level, it will occur a dislocation of the atoms causing a decrease of the crystallinity degree of the sample. Concluding, the PVDF membranes obtained with the mentioned methods showed a predominance of β-phase that varied from 86 to 94% and that a higher porosity promotes a decrease in the tensile strengths and Young's Modulus.

2.6 CO_2 Supercritical

A supercritical fluid is a state attained whenever a pure component or a mixture are brought to value above the critical values of temperature and pressure, as it is shown on figure 7. This technique has been exploited in chromatography and chemical engineering, particularly as a process of extraction and separation. The supercritical has different applications that goes from metal deposition, etching, photoresist removal and waste treatment [34]. The most common component used is CO_2 since it is inert, non-toxic, cheap and available in high purity [35]. Another major advantage of using CO_2 supercritical technique is the low critical point values of CO_2, which are 31.1ºC and 73.8 bar [36]. Whenever these critical points are achieved there is not distinction between the different the liquid and gas phases. These characteristics make the CO_2 the most desired option to be considered as a solvent.

As the critical temperature approaches the *Tcritical*, the density of the gas at the equilibrium becomes denser and the density of the solution decreases. At the critical values, the CO_2 and the solution become one fluid phase.

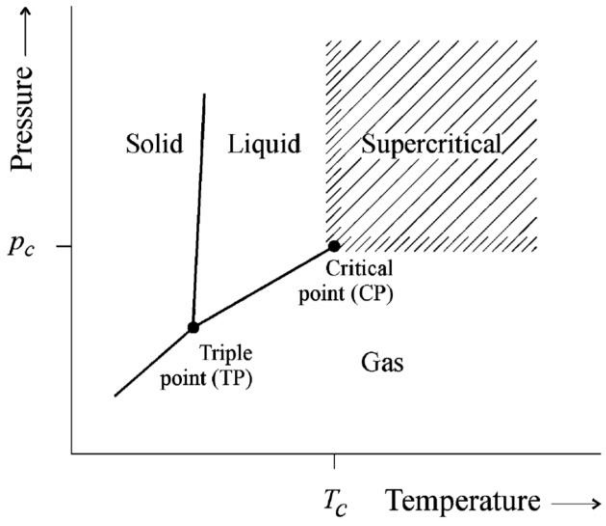

Figure 7 – Example of a phase diagram for a pure component [37].

The membranes were produced with CO_2 assisted phase inversion method [36]. In this method CO_2 will act as an antisolvent that will be immersed on the solution containing the dissolved polymer. Then, the rapid exchange of the solvent and nonsolvent will result in a diffusion-induced phase separation.

During the preparation of membranes, some solvents can present toxic properties that affect the outcome of the membranes. Since, the objective is creating membranes that can be used as a biomaterial, the supercritical CO_2 will be used as an inversion method where it will remove the toxic solvent used to prepare the membrane. This technique is performed under a closed system flow where by manipulating the temperature and pressure of the material will enable the solubilization of the material of interest to then selectively extract it. The sample is placed in the extraction vessel to the be pressurized, so that when the depressurization occurs, the material precipitates without the unwanted solvent.

3

Materials and Methods

3.1 Membrane fabrication

3.1.1 Solvent Casting and particulate leaching

PVDF scaffolds are going to be produced by using solvent-casting and particulate leaching method which is one of the most common techniques used to produce 3D scaffolds in tissue engineering. The major advantage of this technique is the possibility of creating polymer membranes with controlled porosity, pore size and crystallinity [37].

Polyvinylidene fluoride (Mw = 534 000 g/mol; #MKBY6618V) is going to be dissolved in a Dimethylformamide (DMF) (1719239 Fisher Chemical) solution of 10% and 20% w/v, using a magnetic stirrer to facilitate the process of mixing and then sodium chloride will be added to the solution to act as the porogen agent. The residual solvent will be removed after its evaporation through vacuum drying and then some distilled water is added to remove the salt contained in the membranes.

3.1.2 Supercritical CO_2

Similarly, to the previous method, PVDF is dissolved in a DMF (1719239 Fisher Chemical) solution of 10% and 20% w/v. The solutions were mixed in a heating plate at room temperature throughout 24h to promote a good dissolution. The CO_2 (Air Liquide) has a purity of 99.998%.

In this work, the membranes were produced with CO_2 assisted phase inversion method with the assistance of a high-pressure apparatus inside an aquarium full of water heated until a certain temperature, as it is shown in figure 8.

Before starting the experiment, the high-pressure apparatus should be tested without the samples inside to ensure that the system is isolated and there are no leaks or any clogging. If one of these situations is found, it is important to check the system in order to make sure that the pressure is constant during the production of the membranes.

Also, it should be turned on the cryostat in order to decrease the temperature of the flowing CO_2 and the temperature of the bath must be heated until a temperature until a determined temperature set by the experiment.

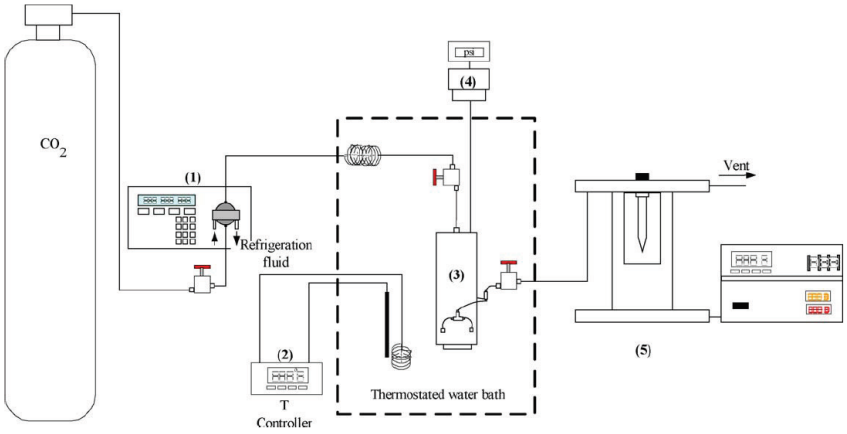

Figure 8 - Layout of the high-pressure apparatus for the membrane formation: (1) piston pump; (2) temperature controller; (3) high-pressure cell; (4) pressure transducer; (5) back pressure regulator [38].

The polymer solution is placed in a vessel inside the high-pressure cylindrical (3) cell made of stainless steel similar to the represented on the schematic displayed on figure 8. Right above the vessel with the polymer solution, there is a disk structure full of porous that will serve as support for the placement of rashig rings, a ceramic porous structure. This is responsible for a better CO_2 distribution upwards toward the output of the cell that is located at the top of the cell.

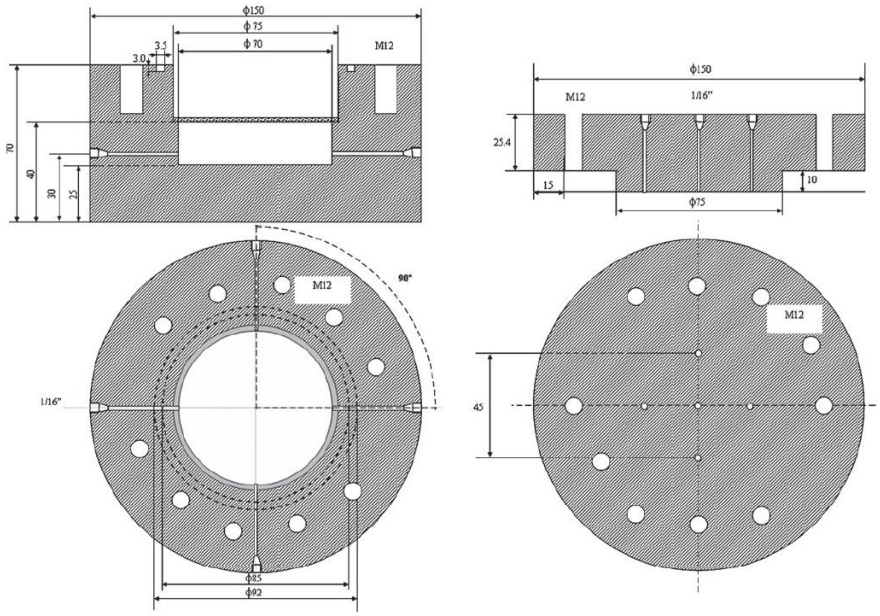

Figure 9 – Schematic representation of the high-pressure cell for membrane preparation [39].

The conditions used for the production of each membrane were the same only changing one variable that was the temperature of the bath where the high-pressure cell is placed, which was 40 ºC or 50 ºC.

To begin the membrane, 0,4 mL of the polymer solution is added to the vessel and the cylindrical cell is placed in a bath at heated temperature initially at 50 ºC, but then the value was changed to 40 ºC since it was the optimal temperature value. The apparatus will be put under a closed system flow where the flow rate of the CO_2 was always 10 g/mL. The pressure in which the process occurred was 186 bar. This value was maintained due to help of the back-pressure regulator. After these parameters were met, the system would be in continuously flow for a period of 2h. At the of the procedure, the system needs to be fast depressurized in a short period of time of about less than 2 minutes.

3.2 Membrane Characterization

The characterization of the membranes was performed by different techniques including scanning electron microscopy (SEM), energy-dispersive X-ray spectroscopy (EDS), X-ray diffraction (XRD) and fast-transform infra-red (FTIR), all available at CENIMAT-I3N.

3.2.1 Scanning electron microscopy (SEM)

The membranes were coated with a thin gold layer using a sputter coating and their morphology and porous' dimension was analysed using a scanning electron microscopy (FIB-SEM) Zeiss Auriga with an acceleration of 5 kV at CENIMAT.

3.2.2 Energy-dispersive X-ray spectroscopy (EDS)

The scanning electron microscopy (FIB-SEM) Zeiss Auriga was also able to perform energy-dispersive X-ray spectroscopy (EDS) through an additional feature Oxford XMax 150 providing a qualitative and a semi quantitative analysis of the elements present in the membranes.

3.2.3 X-ray diffraction (XRD)

The samples were characterized with the diffractometer system XPert-Pro from PANalytical in order to study the crystalline structure of the membranes produced. In these measurements, it was utilized $Cu_{K\alpha}$ radiation with a wavelength of 0.154 nm, an electrical current of 40 mA and a voltage of 45 kV. Also, the samples were characterized with a step of $2\theta = 0.025º$.

3.2.4 Fast-transform infra-red (FTIR)

The chemical structure and the phase present in the samples were characterized with fast-fourier infra-red spectroscopy with a Thermo Nicolet 6700 Spectometer. The measurements were made using an Attenuated Total Reflectance (ATR) and the spectra was obtained with a 45º incident angle in a range from 4000 to 400 cm^{-1} with a resolution of 0.5 cm^{-1}.

3.2.5 Differential Scanning Calorimetry (DSC)

The thermal analysis was performed by TGA-DSC STA 449 F3 Jupiter available at CENIMAT in order to measure the difference in the amount of heat required to increase the temperature of the sample. The analysis was performed in an nitrogen environment of a PVDF sample of 4,6 mg heated from 20 ºC to 220 ºC

3.3 Thermal Stimulated Discharge Current (TSDC)

The TSDC equipment was used to study the polarization of the samples using an electrometer (Keithley 617) connected to a computer that read the data with the help of *Matlab* software. The samples are heated from room temperature until 120 ºC at a rate of 5 ºC/min. After reaching this temperature, an electrical field is applied with the temperature at 120 ºC (Tp) for a period of 30 minutes (tp) in order to orientate the mobile entities. After that time, the temperature decreases until the room temperature and only after this step the electrical field is shut down, as it is seen on figure 10 [14]. This prevents the reorientation of the mobile entities and keep the samples polarized for them to be studied in the cell culture and bioactivity testes. This procedure is what it is called DC poling. The sample gets polarized positively or negatively, depending on the applied voltage that was applied after reaching the temperature of 120 ºC. If no field is applied the sample undergoes just thermal treatment. This equipment is also used to measure the depolarization currents after heating a previously polarized sample. In this situation after cooling down and switching off the electric field, the samples is kept at room temperature for at least the same time that was at Tp, after electrical current is measured while the sample is heating at constant rate. [14]

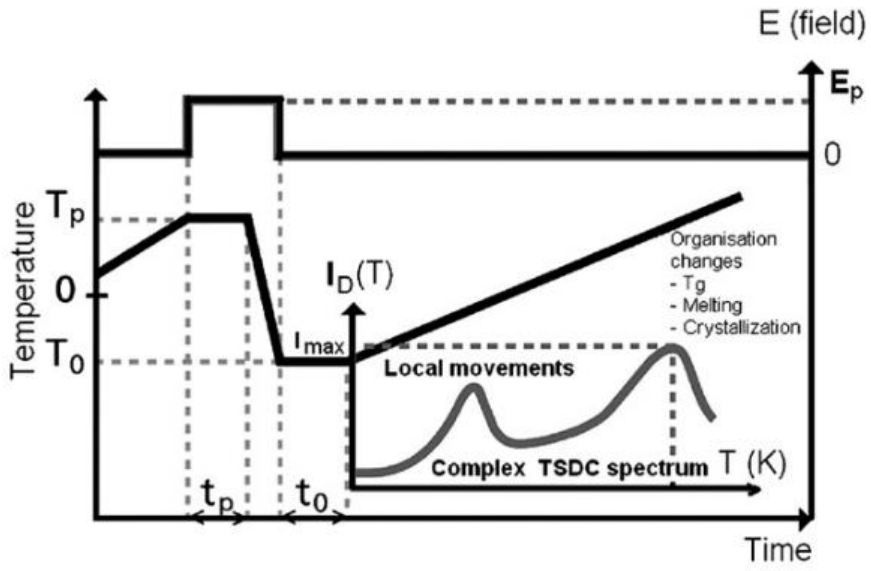

Figure 10 – Sketch of TSDC measurements [14].

3.4 Bioactivity Tests

A bioactive material is one which has been designed to induce specific biological activity according to ESB consensus conference of 1987 [40]. Since it is essential for a material to bond to with the living body, it is used a simulated body fluid (SBF). This fluid possesses ion concentrations equal to those present in the human blood plasma and it will reproduce the in vivo apatite formation on a material. This interaction will occur when the material is immersed in a serum solution.

In this work, a SBF x 1,5 was prepared by using a beaker with 700 mL in a magnetic stirrer at 200 rpm and keeping the pH meter on to control the pH. Then it was added one reactant, one by one, in the proper order while waiting for the previous to dissolve. The reactants were, respectively: 9.8184 g NaCl, 3.4023 g $NaHCO_3$, 0.55591 g KCl, 0.2129 g Na_2HPO_4, 0.4574 g $MgCl_2 \cdot 6H_2O$, 15 mL 1M HCl, 0.5822 g $CaCl_2 \cdot 2H_2O$, 0.1080 g Na_2SO_4 and 9.0945 g Tris. After the dissolution of the last reactant, it is added drop by drop a 1 M HCL until the pH is close to 7.4. When this point is reached, last step is adding Millipore water until the volume is 1 L. After this procedure, the SBF should be kept in the fridge to then to later be used.

Each sample was immersed in a solution with a volume that was calculated through equation 3.1, where A_S is the sample's surface area and the V is the solution's volume [41].

$$0.1\ cm^{-1} = \frac{As}{V} \qquad 3.1$$

The samples were organized in three sets divided periods of 1 day, 2 days and 5 days. In each set there was a sample only heated until 120 ºC, a positive polarized and a negatively polarized sample. For each sample, it was only need 5 mL of SBF.

3.5 Cytotoxicity Tests

Cytotoxicity tests are a method of testing the biocompatibility of the membranes so that these can act as a biomaterial. The current tests were conducted according to ISO 10993-5 standard using the extract method. These standards present a number of test methods designed to evaluate the acute adverse biological effects of extractables from medical devices [42]

The culture medium consisted of DMEM (Dulbecco′s Modified Eagle′s Medium, Sigma-Aldrich #D5030) supplemented with 1.0 g/L D-glucose (Gibco, #15023-021), 3.7 g/L sodium bicarbonate (Sigma-Aldrich, #S5761), 1% GlutaMAX™ (L-alanyl-L-glutamine dipeptide, Life Technologies, #35050-038), 1% sodium pyruvate (Gibco, #11360039), penicillin (100 U/ml) and streptomycin (100 µg/mL) (Invitrogen, #15140122) and 10% FBS (Fetal Bovine Serum, Invitrogen, #10270106).

A membrane of 180 mg was put in 900 µL of medium without containing FBS and was incubated at 37 ºC for a period of 48h. Then, 10% FBS was added and the extracts were added to a previously prepared Vero (epithelial cells from monkey's kidneys) cell cultures. Serial dilutions by a factor of 2 were also added to replicate wells. A positive control was set by adding a cytotoxic compound, dimethyl sulfoxide, to the culture medium and a negative control was set by culturing cells in a normal medium. The cell culture was incubated for 48h. In order to evaluate the cellular viability, extracts and control wells' media were replaced by a resazurin solution consisting of 50% of the culture medium and 50% of resazurin solution prepared at 0.04 mg/mL in PBS (Phosphate Buffered Saline). Resazurin is a metabolic indicator of cell viability that is reduced to resorufin by viable cells.

The ratio of absorbance is read at 570 nm (absorbance maximum of resorufin) and 600 nm (absorbance maximum of resazurin) using a spectrometer ELx800 from BioTek with an absorbance microplate reader.

4

Results and discussion

4.1 Optimising membrane fabrication

PVDF and its copolymer scaffolds produced by using solvent-casting and particulate leaching were produced with 10% and 20% (w/v) concentration using DMF as solvent. The samples produced with this method resembled more like a PVDF film than a membrane. Also, the porosity which is an important factor for this work was not met since the interconnected pores should have a order of magnitude in the order of micrometers, as it is seen in the SEM images shown in figure 11.

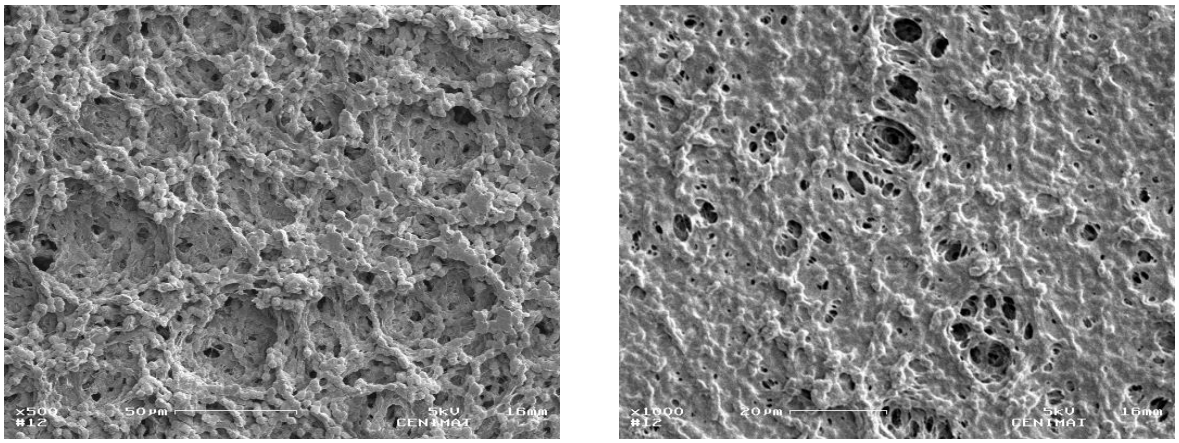

Figure 11 – SEM images at 1000x amplification of PVDF membranes obtained from solvent casting and particulate leaching. The left image is a PVDF membrane with a concentration of 10%, shown at a magnification of 500x and the right has a concentration of 20% shown at a magnification of 1000x.

Besides the necessity of porosity in these membranes, another important factor is the presence of interconnected porous and this was not achieved through this process. A solution found to produce the PVDF membranes was using a supercritical CO_2 method instead of the previous one. With supercritical CO_2 membranes both PVDF and PVDF-TrFe were produced at both concentrations but it was chosen to focus only on the 10% concentration. The reason for that is that as the concentration of the polymer increases, the membrane structure becomes denser and compact. This will lead to a membrane with a low porosity when compared with another produced from a lower concentration solution [43]. This fact is relevant when the membrane is planned to act as a biomaterial and the human tissue needs to interact with an interconnected structure.

After choosing the proper concentration of the membranes, the process of production PVDF membranes was optimized following the conditions already described in the experimental procedure. Unfortunately, the conditions for the PVDF copolymer, PVDF-TrFe, were never met and the membranes fabricated had irregular surface areas that made it impossible to study their properties. A visual comparison between both polymers' membrane can be seen on figure 12.

After these conclusions, the main focus of this work is the study of PVDF membranes obtained with a concentration of 10% (w/v).

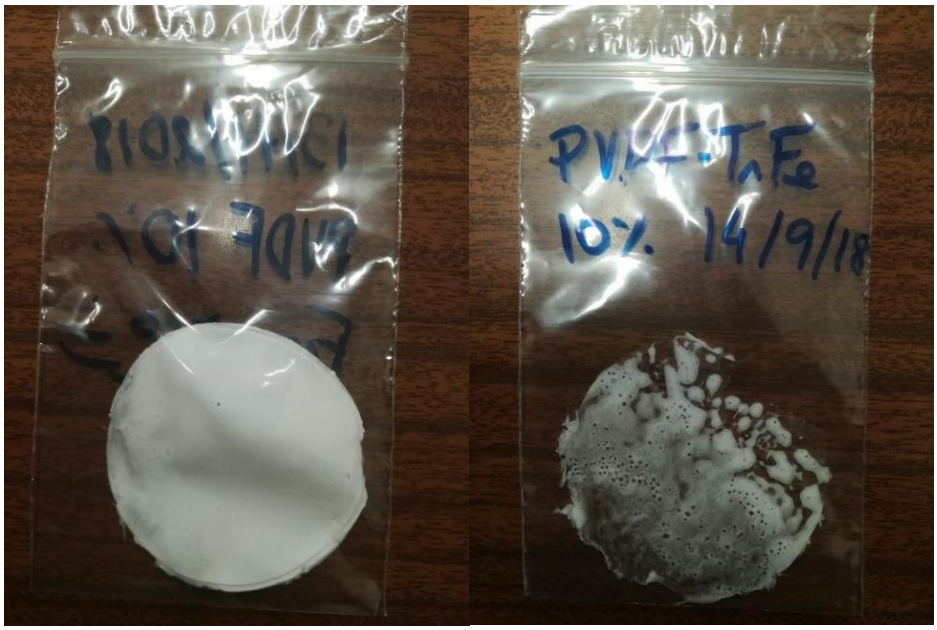

Figure 12 – Comparison between PVDF and PVDF-TrFe membranes superficial structure produced by supercritical CO2. The left image is a PVDF membrane with the optimal structure and the right image is the PVDF-TrFe with the irregular structure.

4.2 Scaffold Characterization

4.2.1 XRD results

The PVDF exhibits four different phases (α, β, γ and δ) that corresponds to different peaks at a diffractogram. Since the objective of this work is the study of piezoelectric properties of PVDF and this is evidenced mainly on β-phase, the samples obtained from the PVDF membrane were analysed using a X-ray diffraction technique. The following data presented on figure 13 was analysed with *OriginPro 9* software and compared with a pure PVDF X-ray diffractogram. Also, it is possible to spot a dominant peak at $2\theta = 20.7°$, that is a characteristic peak of β-phase (2 0 0) [44]. Through this comparison it is possible to assume that the β-phase is present in the membrane.

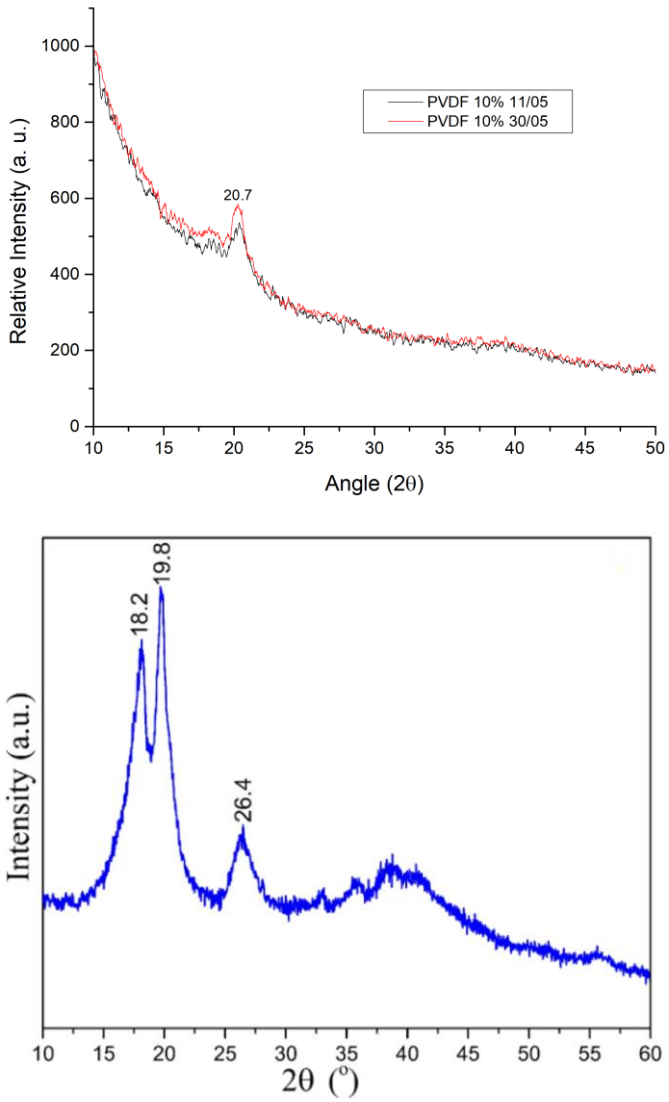

Figure 13 –XRD diafragtogram of two different PVDF membranes produced through supercritical CO_2, on the left graph. The right graph is a XRD of PVDF in raw powder [45].

4.2.2 DSC results

Comparing the results obtained from DSC analysis from the PVDF powder and the samples obtained from the membranes produced, we can observe in figure 14 that the peak of the melting temperature was practically the same for both, around 160 ºC.

The DSC scans also made possible the study of the crystallinity which could be obtained using equation 4.1 [46].

$$X_C(\%) = \frac{H_{fs}}{H_{ft}} * 100 \qquad 4.1$$

The H_{fs} corresponds to the area beneath the primary melting peak in the upper graphic of figure 14 and the H_{ft} corresponds to fusion enthalpy of a 100% crystalline sample. The X_C obtained was 23.83 %.

Also, there was a small difference in the TG %, resulting on a mass change of 3.54 %.

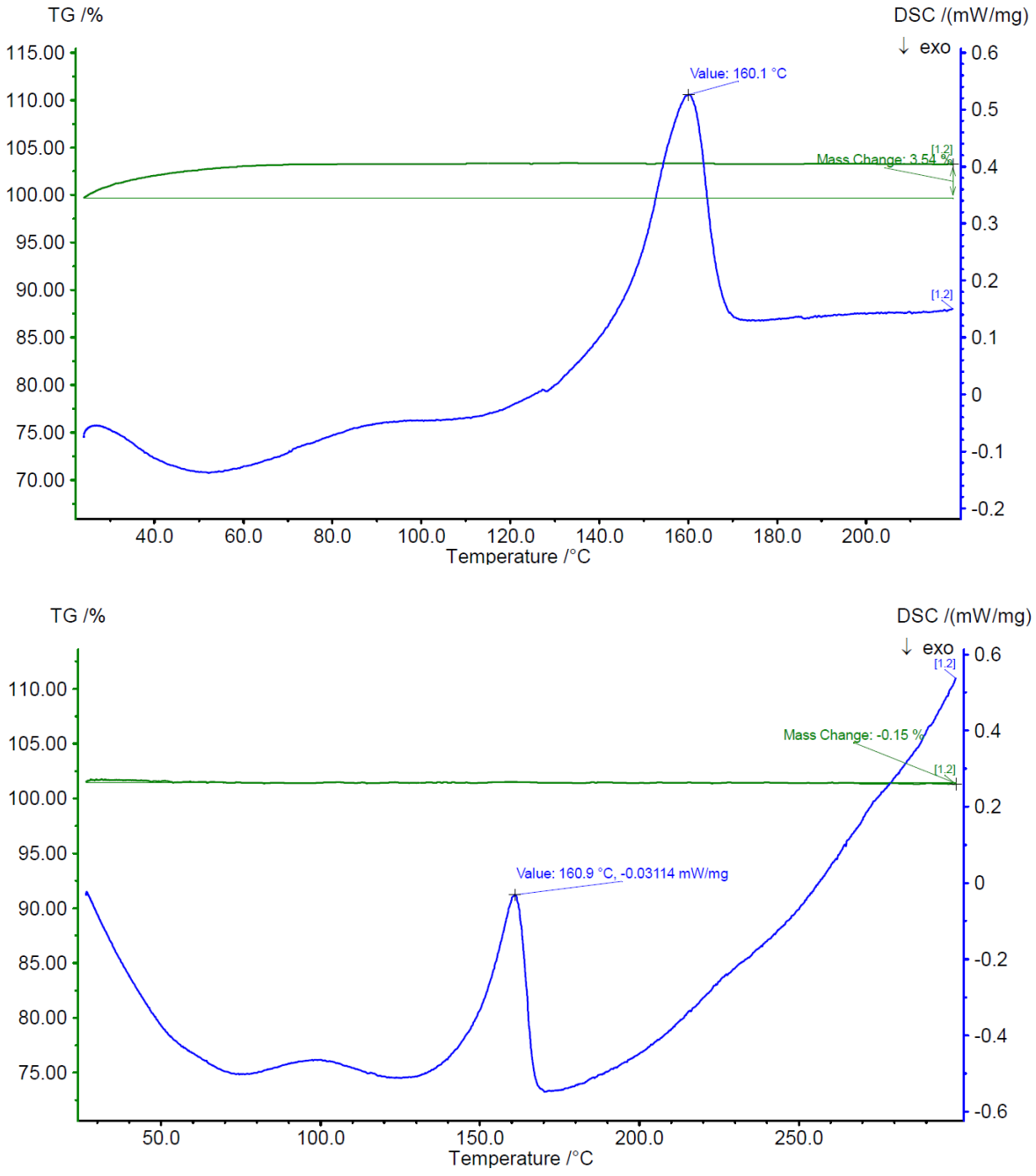

Figure 14 – DSC analysis of a PVDF membranes produced through supercritical CO_2, on the upper graph. The bottom graph is a DSC of PVDF in raw powder.

4.2.2 FTIR results

The FTIR spectra was analysed for two different PVDF membranes and several peaks were detected. In figure 15, it is seen α-phase characteristic peaks and β-phase peaks. For α-phase, the most evident are the 614, 763, 796, 867, 870 cm^{-1} and the β-phase are located at 510, 840 and 1278 cm^{-1} [47].

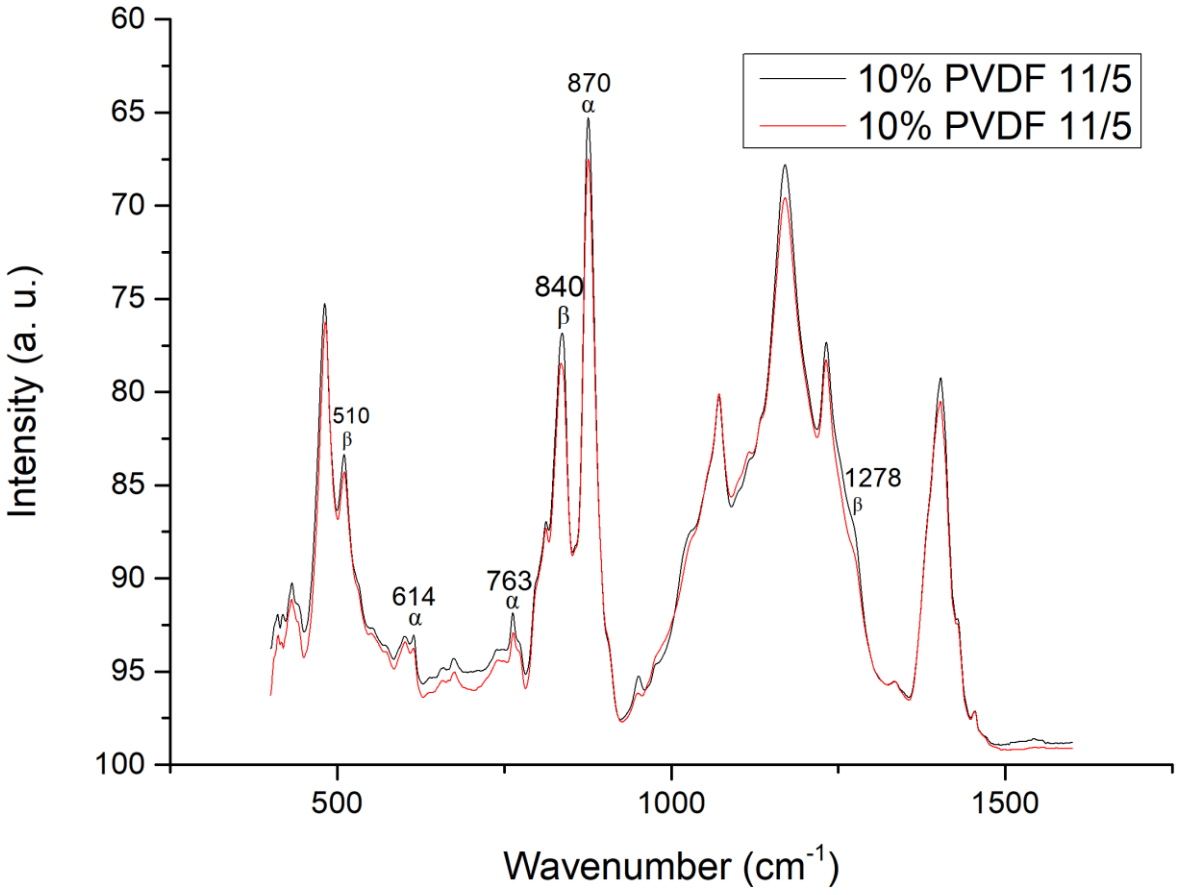

Figure 15 – XRD spectre of two different PVDF membranes produced through supercritical CO_2.

4.2.3 TSDC

A thermal stimulated depolarization current technique was used to measure the dielectric properties of the samples. This way the sample could be positive and negatively polarized in order to study the effect of the electric field on piezoelectric samples. Figure 16 shows the effect of thermal treatment and positive and negatively polarization.

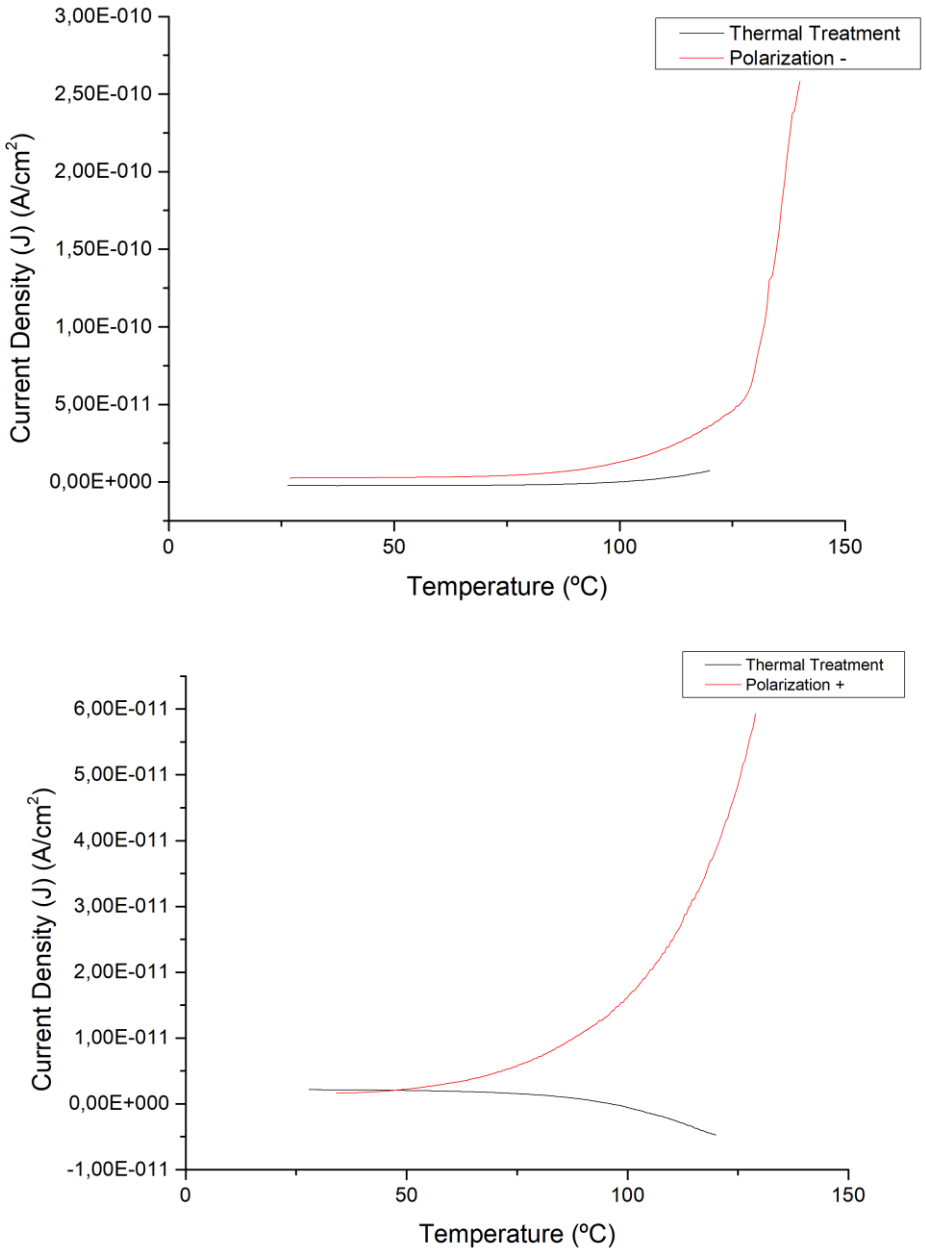

Figure 16 – Comparison between the current density of negative (left graph) and positive (right graph) depolarization on a membrane of thickness of 300 µm with an electric field of 400 kV/m, t_p = 0.5h and T_p = 120 ºC.

All the samples with a thickness of 300 µm were heated until 120 ºC at a rate of 5 ºC/min and the electric field applied was 400 kV/m for a period of 30 minutes. Then after switching off the field, the samples were tested to check the effects on the samples. By analysis of figure 17, the magnitude of current density increased in both positive and negative polarizations as the temperature increased. The positive polarization showed a higher increase of current density when compared to negative polarization. Also, the highly increasing slope in the negative polarization at temperature

near end temperatures might suggest a degradation on the PVDF, as it is confirmed on the DSC with the melting temperature close to 160 ºC.

Another comparison made was studying the difference of thickness with three different samples negatively polarised with different thicknesses of 280, 290 and 300 µm as it is shown in figure 15. There was a relevant difference in the current density on the 290 µm sample.

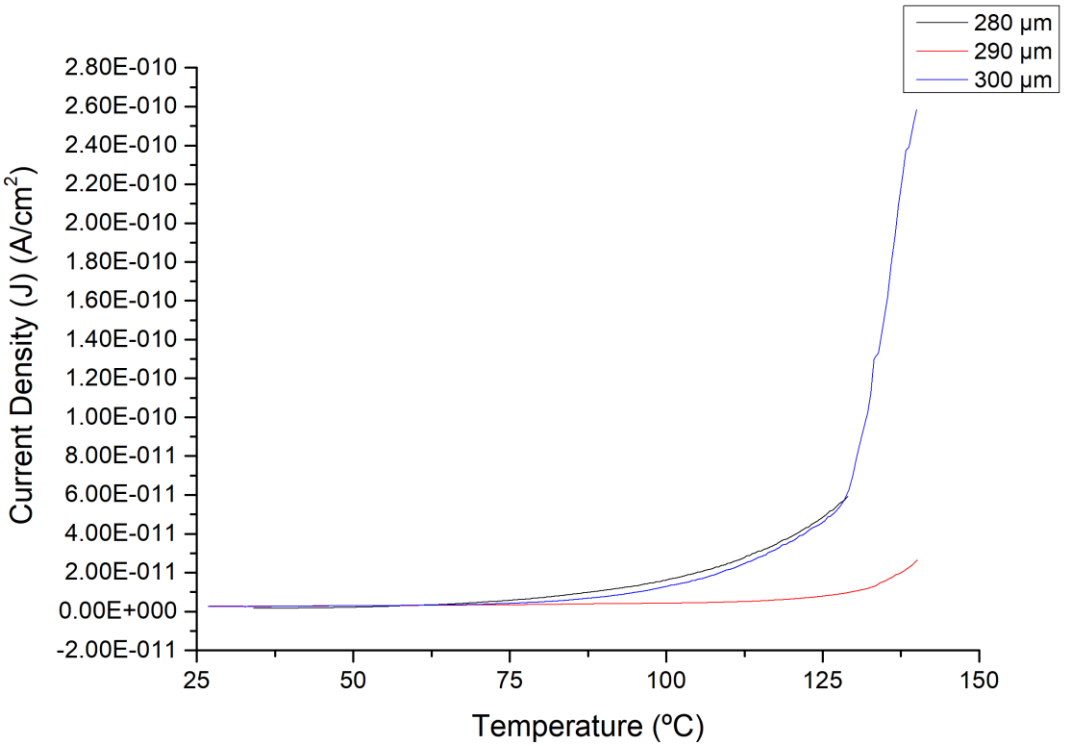

Figure 17 – Comparison of current density of membranes with different thicknesses with an electric field of 400 kV/m.

4.3 Microscopical Analysis

The samples from the PVDF 10% membranes analysed with SEM have provided information about the scaffold's structure. It is shown different magnifications: 1k x, 5k x, 10k x and 20k x. The PVDF 10% membranes produced by supercritical CO_2 displayed an interconnected pore structure as it is seen in figure 18.

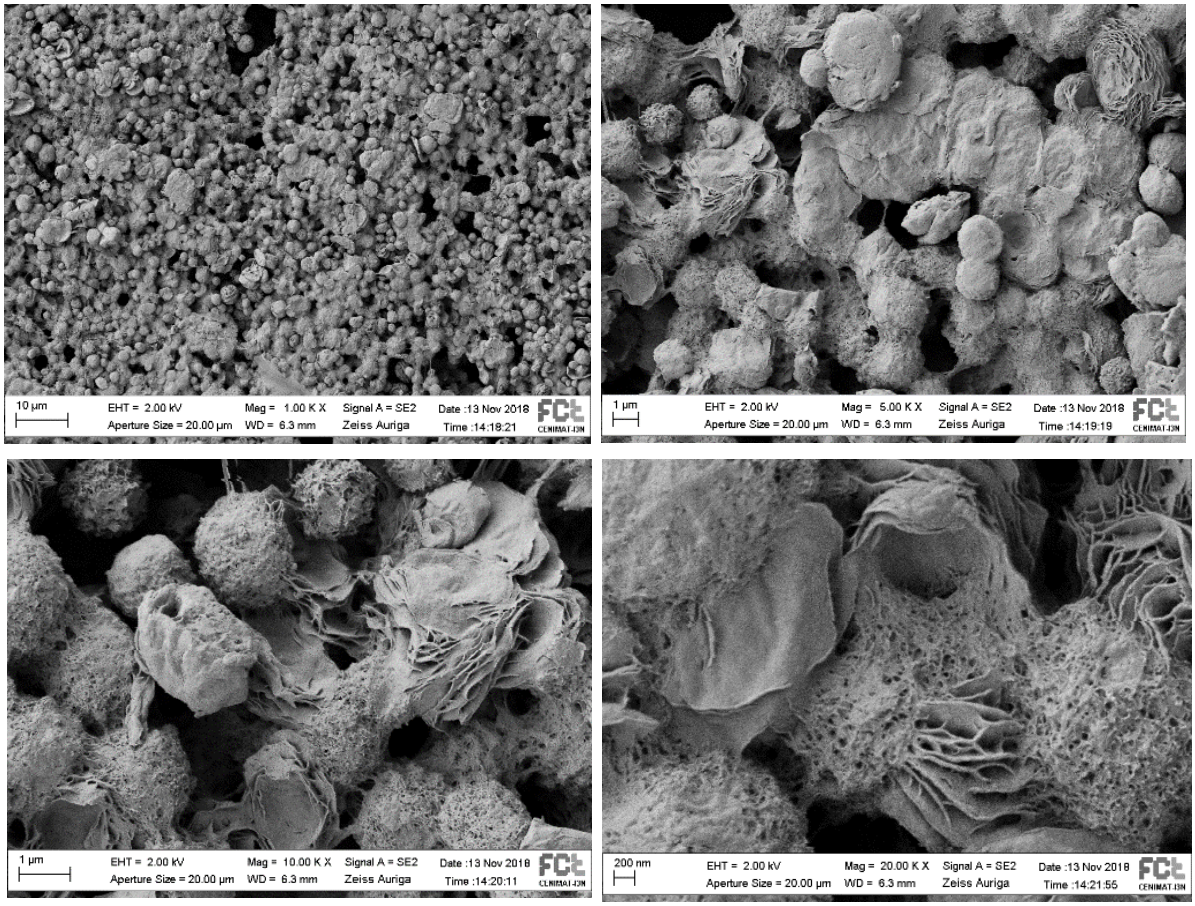

Figure 18 – Top view of a PVDF 10% membrane at 1k x, 5k x, 10k x and 20k x magnification.

The top superficial area displayed a spherulitic crystallization across all the sample due to the release of the CO_2 during the fast depressurization step during the production of the membrane. Also, as it is said above, it is possible to confirm the presence of interconnected pores. Despite that, this view is not the best to understand the dimension of the pores.

The bottom superficial area shown on figure 19, in contrast with the previous one, is flat across all membrane since it is in contact with the vessel where the PVDF 10% (w/v) solution is placed. During the depressurization, the CO_2 flows out of the system upwards leaving the bottom superficial area with lesser pores visible.

The cross-section area in figure 20 provides information about the inner structure of the membrane. Unfortunately, the section wasn't cut with liquid nitrogen which deformed the edges of the sample. Still, it was possible to understand the morphology of the structure.

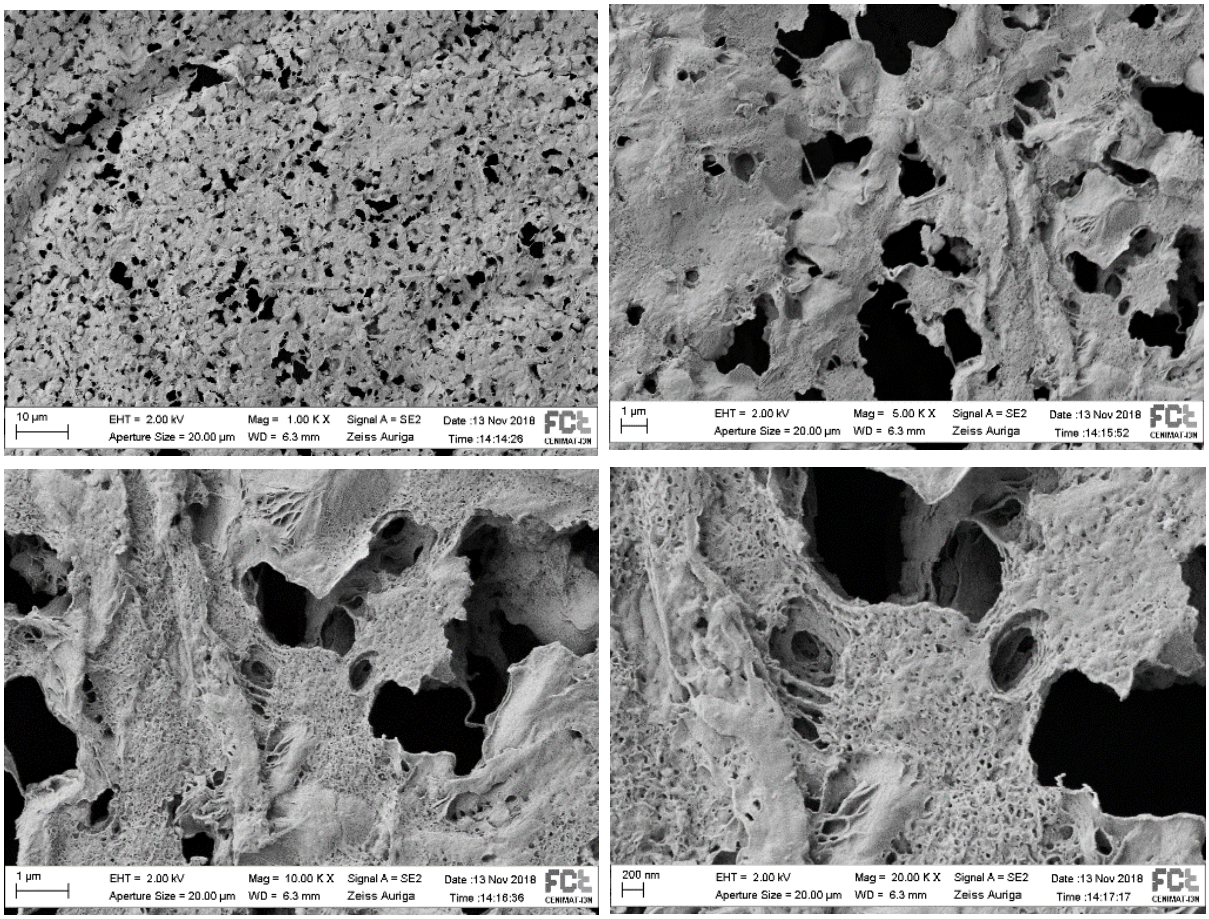

Figure 19 – Bottom view of a PVDF 10% membrane at 1k x, 5k x, 10k x and 20k x magnification.

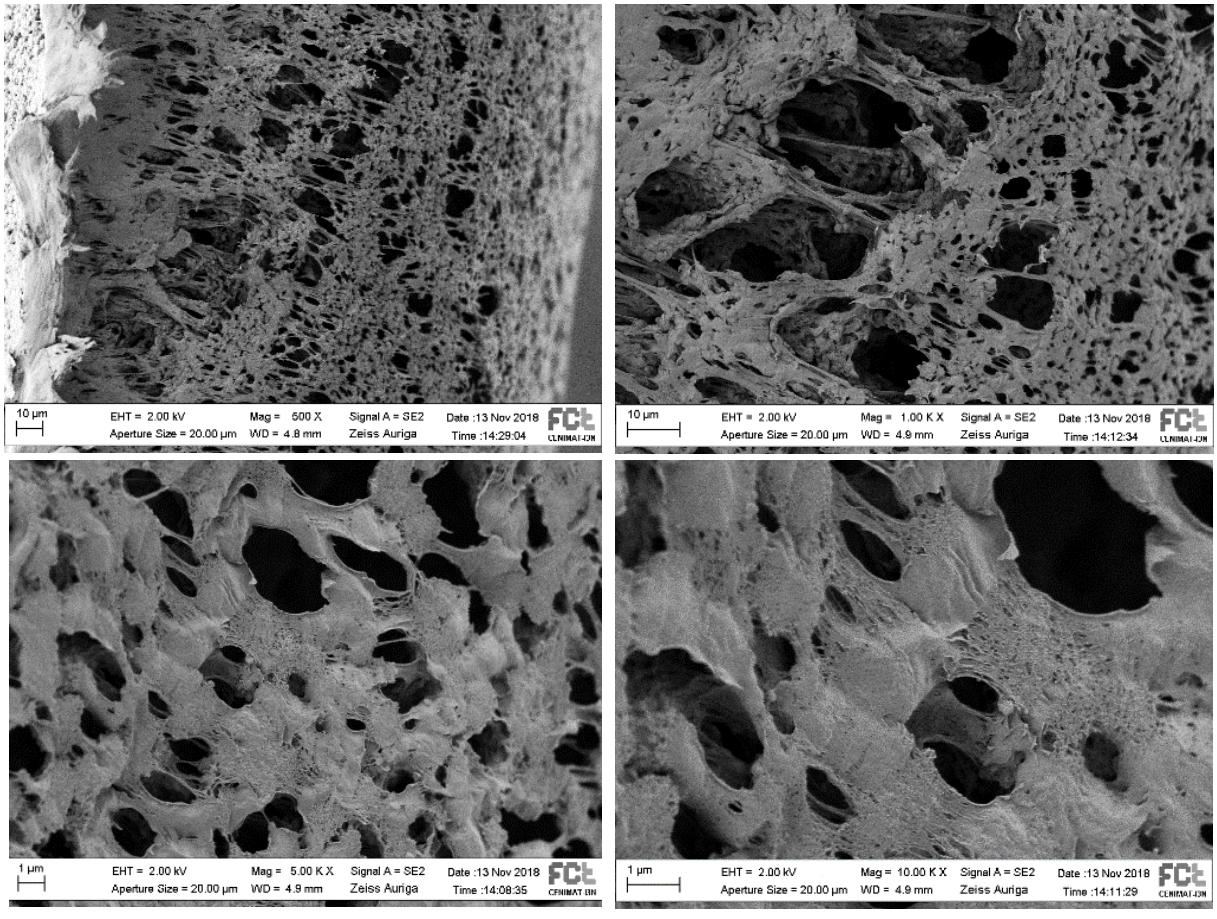

Figure 20 – Cross-section view of a PVDF 10% membrane at 500 x, 1k x, 5k x and 10k x magnification.

The dimensions of the pores have different sizes but in regions where the scaffold was not deformed by the cut, the size, considering that the pore has a spherical structure, is ranging around 1 to 5 µm in diameter. The average dimension of an osteocyte cell is ranging around 5 to 20 µm [48].

The porosity was also calculated through equation 4.2 where p_{PVDF} is the density of different samples obtained from the membranes produced from supercritical CO_2 and $p_{PVDFdense}$ is the density of a dense membrane produced by pouring the PVDF 10% (w/v) into a glass plaque that was left to dry at 37 ºC during 24 hours in order to form a dense membrane.

$$\text{Membrane porosity (\%)} = \left(1 - \frac{p_{PVDF}}{p_{PVDFdense}}\right) * 100 \qquad 4.2$$

In these tests, p_{PVDF} was obtained by an average of 8 samples of different thicknesses and the result obtained for the membrane porosity was (76.5 ± 0.1) %.

4.4 Bioactivity Tests

Besides the structural analysis, bioactivity tests were done to evaluate the interaction of the polymer with immersion in SBF for periods of 1 day, 2 days and 5 days. For each of these periods, the 3 different samples were tested: one that was thermally treated, a negatively polarized and a positively polarized. It is important to state that the post treatment samples weren't washed with distilled water which caused the appearance of some salts such as NaCl and KCl in the SEM images.

4.4.1 Thermal Treatments samples

Figure 21 displays a comparison between the morphology of thermal treatments samples at a magnification of 10k x through SEM image. It is possible to confirm that as the period of time increased, the deposite layer of salts ending up to cover the PVDF membrane. This fact is more noticeable when the 24h sample is compared with the 5-day sample. In this last one, the presence of salt crystals is also more noticeable than the other two samples. The EDS report for the 1-day sample and the 5-day can be found in annex 1 and 2, respectively. In the 1-day report, the $\frac{Ca}{P}$ relation was 0.94 and in the 5-day sample the $\frac{Ca}{P}$ relation was 0.78.

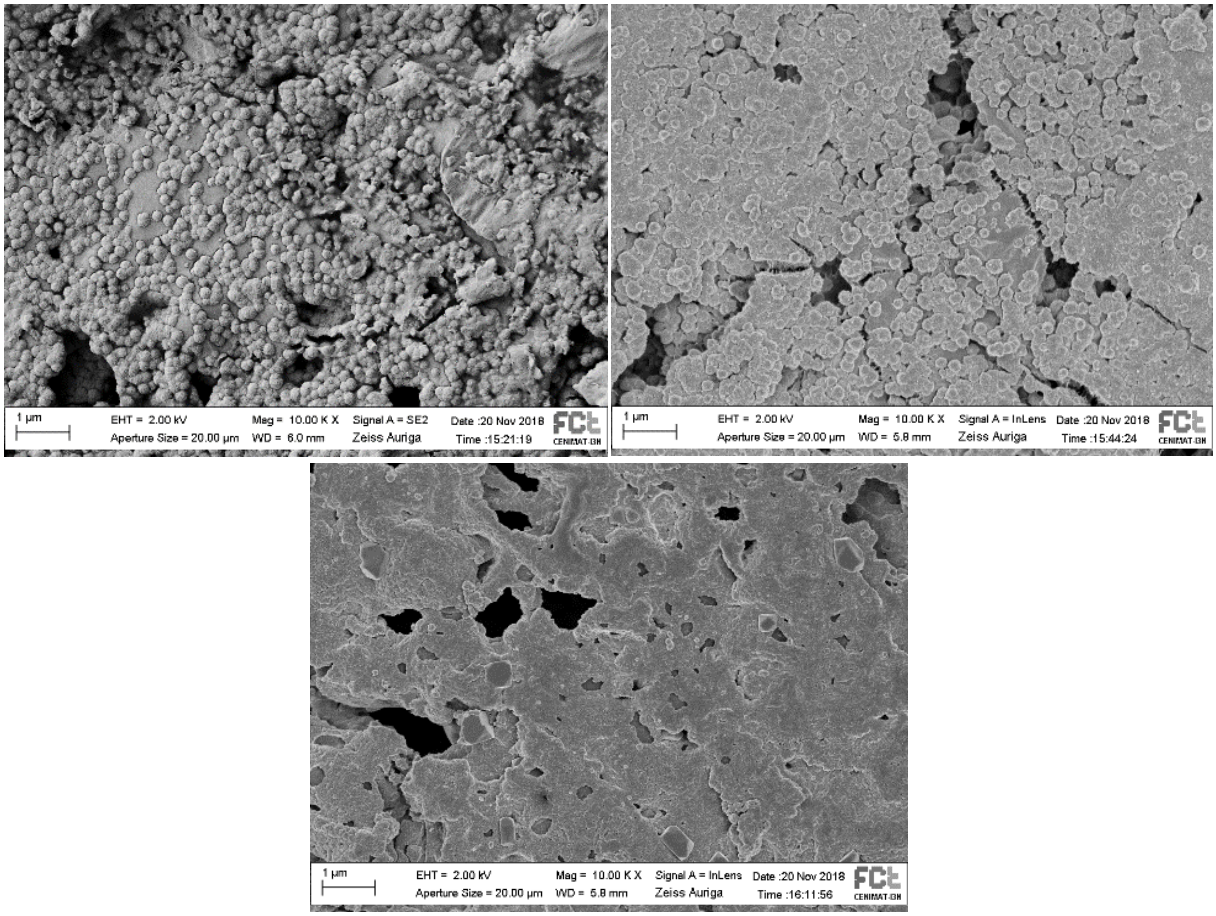

Figure 21 – Top view of a PVDF 10% membrane at magnification of 10k x subjected to a thermal treatment for 24h, 48h and 5 days immersed in SBF, respectively.

4.4.2 Positively polarized samples

In the positively polarized samples, shown on figure 22, the pattern remains the same since the deposition on the PVDF surface increased significantly when comparing the 24h sample and the 5-day sample. Also, the presence of the salt crystals is higher than in the sample without polarization which indicates an affinity between the presence of positive polarized charges in surface of the membrane. The EDS report for the 1-day sample and the 5-day can be found in annex 3 and 4, respectively. In the 1-day report, there was also no Ca and P ions but in the 5-day the $\frac{Ca}{P}$ relation was 0.46, a lower value than the one obtained without any kind of polarization.

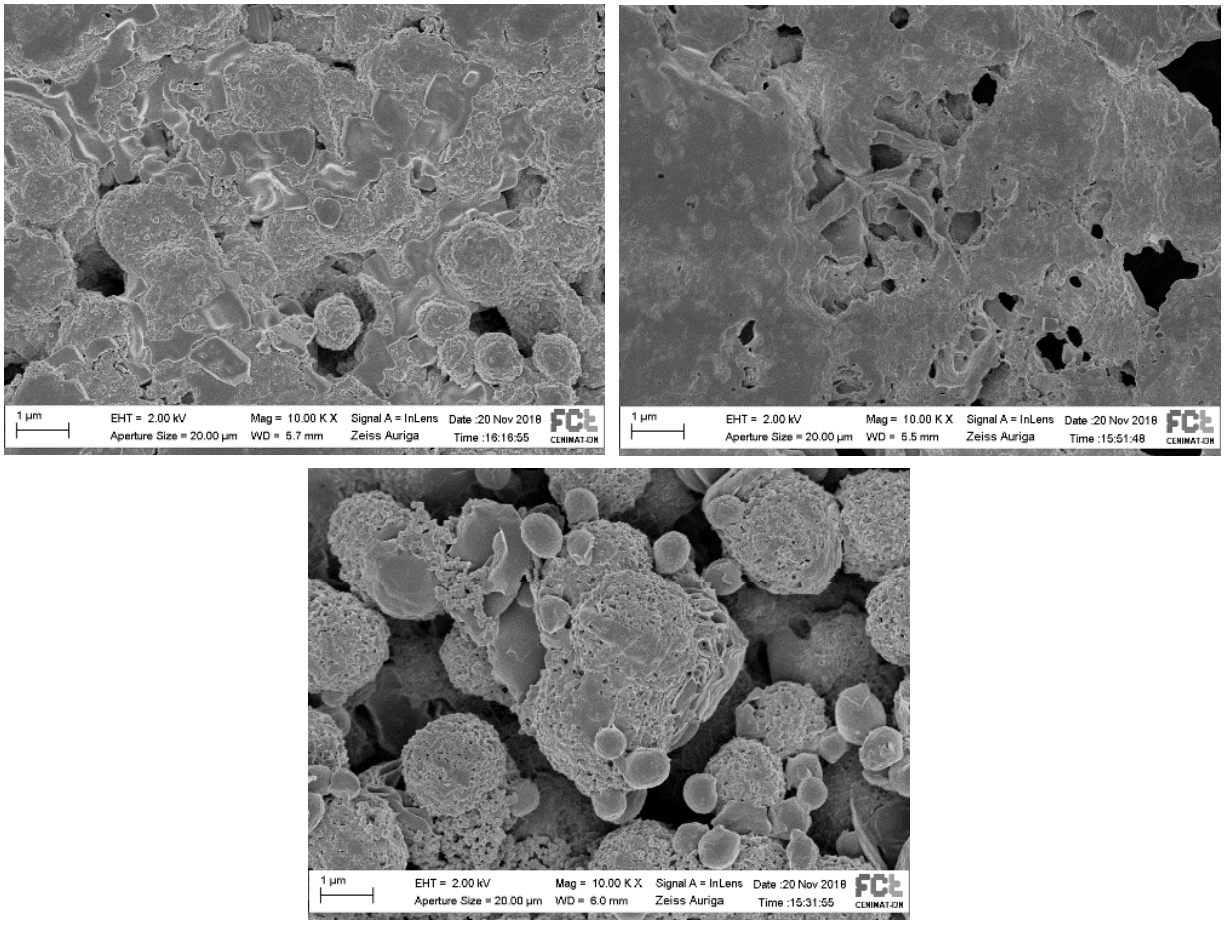

Figure 22 – Top view of a PVDF 10% membrane at magnification of 10k x subjected to a positively polarization for 24h, 48h and 5 days immersed in SBF, respectively.

4.4.3 Negatively polarized samples

In the negative polarized samples, shown on figure 23, the deposition on the PVDF surface increased in the same way of the previous samples. Besides, the presence of the salt crystals is higher than in the sample without polarization but it is lower when compared to the positively polarization. The EDS report for the 1-day sample and the 5-day can be found in annex 5 and 6, respectively. In the 1-day report, unlike the previous samples, there was a small $\frac{Ca}{P}$ relation of 0.013 and in the 5-day this relation increased to 0.35, the lowest value of the 5-day samples.

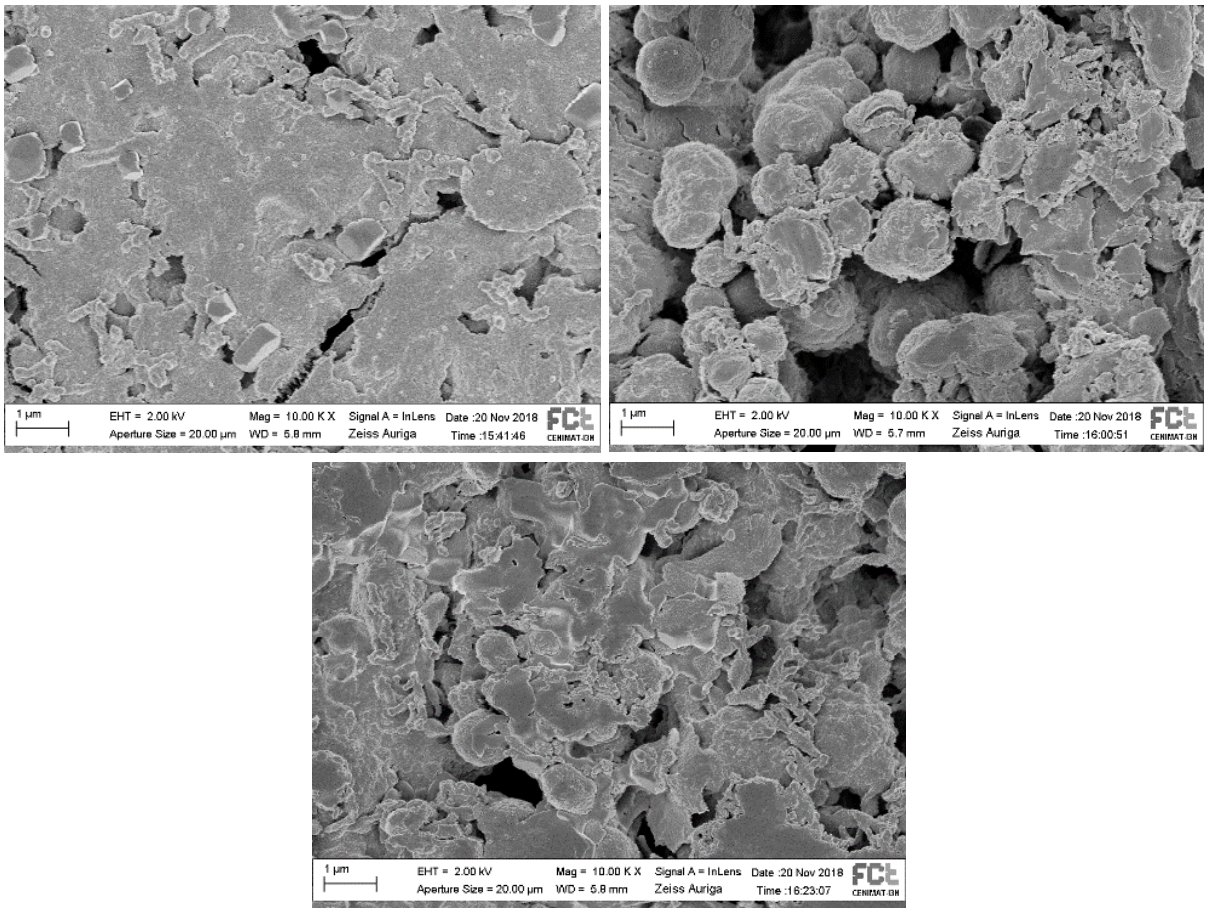

Figure 23 – Top view of a PVDF 10% membrane at magnification of 10k x subjected to a negatively polarization for 24h, 48h and 5 days immersed in SBF, respectively.

In the different annexes, EDS provided the elements contained in the analysed samples which were PVDF's atoms (C and F), as it was expected, and some atoms such as phosphorus and calcium. These were in higher quantities since the samples reacted to the induced interaction with the surface guaranteeing the bioactivity of the PVDF membranes.

4.5 Cytotoxicity tests

Cytotoxicity of the membranes was evaluated according to the ISO 10993-5 standard using resazurin as a viability indicator. Resazurin is blue and non-fluorescent reagent that is reduced by viable cells to resorufin that is pink fluorescent. The quantity of resorufin is proportional to the number of living cells so the absorbance values are proportional to the number of living cells.

For each experiment condition, the absorbance is compared with that of negative control (viable cells). For the extract concentrations used (1x, 0.5x, 0.25x and 0.125x), the relative cell viability values obtained (0.98, 1.02, 1.07 and 1.00, respectively) were always higher than 0.9 which

confirms that the PVDF 10% membrane is a non-cytotoxic material. An important factor is guaranteeing that the viability assessment method is in fact sensitive to cell viability. To this purpose, cell population on the positive control (dead cells) was also evaluated and showed a relative cell population of 0.06.

4.6 Adhesion and proliferation test

Samples from three different membranes were seeded with 20 000 osteoblast cells/cm^2 in order to test cell adhesion and proliferation. The proliferation test was performed twice on days 3 to 5 of the culture. There was no difference between the three membranes and the adhesion ratio was (63 ± 5) %. Between days 1 and 3 the proliferation rate was (1.30 ± 0.08) and between days 3 and 5 it was (1.28 ± 0.07).

To image cell distribution on membranes, a fluorescence technique was used. Cell nuclei were imaged with a 4′,6-diamidino-2-phenylindole (DAPI). DAPI is a fluorescent stain that binds to adenine-thymine regions in the DNA. DAPI can pass through the membrane without damaging the cells and is used to visualize the cells' nucleus. In figure 24, it is possible to see an example of the distribution of the cells on the PVDF membrane.

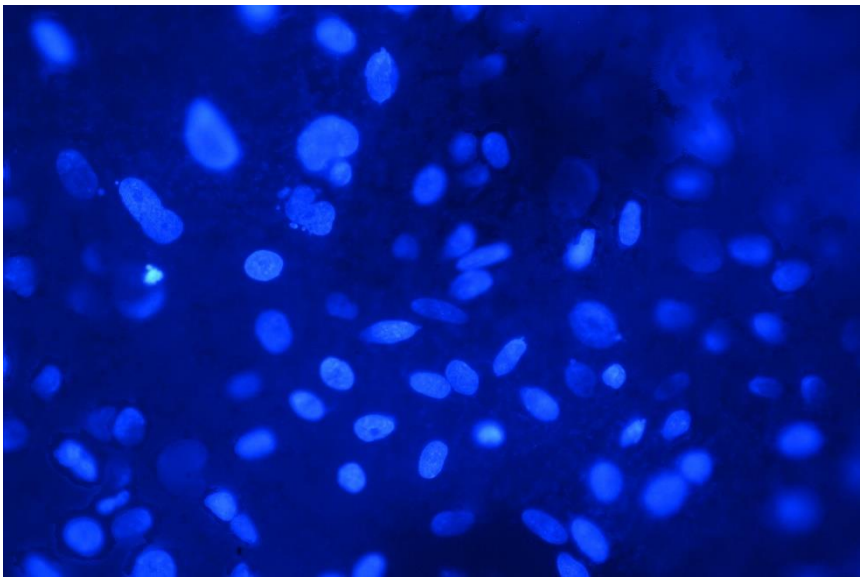

Figure 24 – Example of the cell distribution on a PVDF membrane using fluorescence microscopy with a DAPI stain.

5

Conclusions and future perspectives

The main objective of this work was the production of piezoelectric membranes and the study of its application as a biomaterial. This goal was achieved with the fabrication of membranes using PVDF which is a polymer that exhibits piezoelectric activity in its β-phase. PVDF membranes were successfully produced using a supercritical CO_2 method. The optimal production parameters for these membranes were a 10% (w/v) concentration solution using DMF as solvent, in a bath of 40 ºC and a flowing CO_2 of 186 bar during a period of 2 hours.

All membranes were produced in the same conditions with a regular surface area and a average thickness of 300 µm. The SEM images provided information about the morphology of the internal structure and it was possible to confirm an interconnected porous structure as it was expected from studies in the literature. The porous dimension was on average 5 µm and the EDS results stated that there were no other compounds in the samples other than PVDF. The porosity of the membrane was (76.5 ± 0.1) % and it was obtained by comparing the density of the samples with a dense membrane showing a high porosity structure.

XRD results confirmed the presence of β-phase since the diffractogram displayed a dominant peak at $2\theta = 20.7°$ corresponding to (2 0 0) peak, that is a characteristic peak of this phase. Also, in FTIR spectra it was confirmed several peaks from both α and β-phase, respectively.

DSC results stated the melting temperature of 160 ºC and the mass change during the heating. This value can explain the high increase in the FTIR peak as the temperature approaches the melting temperature. The calculated crystallinity was 23.83 %.

TSDC results stated that polarizing a sample with an electrical field of 400 kV/m heated at 120 ºC for 30 minutes promotes an increase in the current density as the temperature rises. For temperatures above than the one of polarization, the current density increased at a fast rate possibly indicating that the membranes might had suffer a degradation in its structure, as it approaches the melting temperature.

For the bioactivity test, the 3 sets of samples were immersed on a SBF solution for a period of time of 24h, 48h and 5 days. As expected as the time passed by, there was an increase in the deposition of calcium phosphate on the surface. Despite that, the main components of the samples

were the PVDF atoms and in minor quantities as detected Ca and P indicating the deposition of the hydroxyapatite.

Cytotoxicity tests were also successful since the viability ratio for each concentration was above 0.9 guaranteeing that the material was non-cytotoxic and can be used as a biomaterial. For the adhesion tests, no difference was encountered between the three studied membranes, which were thermally treated but not DC poled, and the adhesion rate for them was (63 ± 5) %. Also, for the same membranes, the proliferation ratio was (1.30 ± 0.08) between days 1 and 3 and (1.28 ± 0.1) between days 3 and 5.

In the future, there are several steps to improve in this research. First, the process of production could be optimized for different concentrations of PVDF, while guaranteeing a interconnected porous structure. Another step is the optimization of the PVDF-TrFe production by supercritical CO_2 since this polymer only exhibits β-phase and has a higher piezoelectric response when compared with PVDF. Measuring the piezoelectric constant d33 response and testing the viability of polarized samples would also be a good contribute to this work.

6

References

[1] J. Viola, B. Lal and O. Grad, "The Emergence of Tissue Engineering as a Research Field", National Science Foundation, 2003. [Online]. Available from: https://www.nsf.gov/pubs/2004/nsf0450/emergence.pdf [Accessed: 29/01/2018].

[2] B. Lipinski, “Biological significance of piezoelectricity in relation to acupuncture, hatha yoga, ostheopathic medicine and action of air ions”, Medical Hypotheses, vol. 3 no. 1, pp. 9–12, January-February 1977. DOI: http://dx.doi.org/10.1016/0306-9877(77)90045-7.

[3] J. Huang, Z. Ye, X. Hu, L. Lu and Z. Luo, “Electrical stimulation induces calcium-dependent release of NGF from cultured Schwann cells” *Glia*, vol. 58, no. 5, pp. 622–631, April 2010. DOI: https://doi.org/10.1002/glia.20951.

[4] K. Haastert-Talini and C. Grothe, "Chapter Five - *Electrical Stimulation for Promoting Peripheral Nerve Regeneration", in* S. Geuna, I. Perroteau, P. Tos and B. Battiston, Eds., Tissue Engineering of the Peripheral Nerve Biomaterials and physical therapy, 1st Edition, Academic Press, 2013, pp. 111-124. ISBN**:** 9780124200449. DOI: https://doi.org/10.1016/B978-0-12-420045-6.00005-5.

[5] P. Aebischer, R. F. Valentini, P. Dario, C. Domenici and P. M. Galletti, “Piezoelectric guidance channels enhance regeneration in the mouse sciatic nerve after axotomy” *Brain Research*, vol. 436, no. 1, pp. 165–168, August 1987. DOI: https://doi.org/10.1016/0006-8993(87)91570-8.

[6] D. F. Williams, “The Language of Biomaterials-Based Technologies” *Regenerative Engineering and Translational Medicine*, Springer International Publishing, vol. 4, pp. 1-8, December 2018. ISSN: 2364-4133

[7] F. O'Brien, "Biomaterials & scaffolds for tissue engineering", Materials Today, vol. 14, no. 3, pp. 88-95, March 2011. DOI: https://doi.org/10.1016/S1369-7021(11)70058-X.

[8] GODT, Home - GODT, 2018. [Online]. Available from: http://www.transplant-observatory.org/ [Accessed: 10/11/2018].

[9] UNOS, "Data", UNOS, 2018. [Online]. Available from: https://unos.org/data/ [Accessed: 29/01/2018].

[10] A. Singh and N. A. Peppas, "Hydrogels and Scaffolds for Immunomodulation" *Advanced Materials*, vol. 26, no. 38 pp. 6530–6541, 2014. DOI: https://doi.org/10.1002/adma.201402105

[11] N. B. Patel, Z. Xie, S. H. Young, and M. M. Poo, "Responses of nerve growth cone to focal electric currents" *Journal of Neuroscience Research*, vol. 13, pp. 245–256, 1985. DOI: https://doi.org/10.1002/jnr.490130117

[12] J. Harrison and Z. Ounaies, "Piezoelectric polymers", in J.Kroschwitz and H. Mark, Eds., Encyclopedia of Polymer Science and Technology, 2002. ISBN: 9780471440260 DOI: https://doi.org/10.1002/0471440264.pst427

[13] R. H. W. Funk and T. K. Monsees, "Effects of Electromagnetic Fields on Cells: Physiological and Therapeutical Approaches and Molecular Mechanisms of Interaction", Cells Tissues Organs, vol. 182, no. 2, pp. 59-78, 2006. DOI: https://doi.org/10.1159/000093061

[14] V. Gun'ko, V. Zarko, E. Goncharuk et al., "TSDC spectroscopy of relaxational and interfacial phenomena", Advances in Colloid and Interface Science, vol. 131, Issue 1-2 , pp. 1-89, 2007. DOI: 10.1016/j.cis.2006.11.001

[14] W. D. Callister, Jr., Fundamentals of Materials Science and Engineering, 5th Edition, New York: Wiley, December 2000. ISBN-10: 047139551X

[15] A. Manbachi and R. Cobbold, "Development and Application of Piezoelectric Materials for Ultrasound Generation and Detection" *Ultrasound*, vol. 19, no. 4, pp. 187–196, November 2011. DOI: https://doi.org/10.1258/ult.2011.011027

[16] G. G. Genchi *et al.*, "P(VDF-TrFE)/BaTiO3Nanoparticle Composite Films Mediate Piezoelectric Stimulation and Promote Differentiation of SH-SY5Y Neuroblastoma Cells" *Advanced Healthcare Materials.*, vol. 5, no. 14, pp. 1808–1820, July 2016. DOI: https://doi.org/10.1002/adhm.201600245

[17] D. J. Jones, S. E. Prasad and J. B. Wallace, Piezoelectric Materials and their Applications, Key Engineering Materials, vols. 122-124, pp. 71–144, 1996. DOI: https://doi.org/10.4028/www.scientific.net/KEM.122-124.71

[18] P. A. Downey and M. I. Siegel, "Bone biology and the clinical implications for osteoporosis," Physical Therapy, vol. 86, no. 1, pp. 77–91, February 2006. DOI: https://doi.org/10.1093/ptj/86.1.77

[19] S. R. Goldring, “The osteocyte: key player in regulating bone turnover”, RMD Open 2015, vol. 1, Issue Supply. 1, November 2015. DOI: http://dx.doi.org/10.1136/rmdopen-2015-000049

[20] E. Bonucci, "Chapter Four - The Nature and Composition of the Inorganic Phase", in Biological Calcification: Normal and Pathological Processes in the Early Stages, 1st Edition, Springer, 2013, pp. 67-71. ISBN: 978-3-540-36012-4.

[21] E. Fukada and I. Yasuda, “On the Piezoelectric Effect of Bone” Journal of the Physical Society of Japan, vol. 12, no. 10, pp. 1158–1162, October 1957. DOI: https://doi.org/10.1143/JPSJ.12.1158

[22] D. Rossi and P. Dario, “Biomedical applications of piezoelectric and pyroelectric polymers” *Ferroelectrics*, vol. 49, no. 1, pp. 49–58, February 1983. DOI: https://doi.org/10.1080/00150198308244665

[23] R. Valentini, T. Vargo, J. Gardellajr and P. Aebischer, "Electrically charged polymeric substrates enhance nerve fibre outgrowth In vitro", *Biomaterials*, vol. 13, no. 3, pp. 183-190, 1992. DOI: https://doi.org/10.1016/0142-9612(92)90069-Z

[24] K. Lhoste, Development of PVDF micro and nanostructures for cell culture studies, *PhD.*, Université Paris Descartes, 2012.

[25] H. Kawai, “The Piezoelectricity of Poly (vinylidene Fluoride)” Japanese Journal Applied Physics, vol. 8, no. 7, pp. 975–976, May 1969. DOI: http://dx.doi.org/10.1143/JJAP.8.975

[26] S. Satapathy, P. Gupta, S. Pawar and K. Varma, "Crystallization of Beta-phase Poly (vinylidene fluoride) films using dimethyl sulfoxide (DMSO) solvent and at suitable annealing condition", *Arxiv.org*, 2018. [Online]. Available from: http://arxiv.org/abs/0808.0419. [Accessed: 29/01/2018].

[27] R. Hasegawa, Y. Takahashi, Y. Chatani and H. Tadokoro, "Crystal Structures of Three Crystalline Forms of Poly(vinylidene fluoride)", *Polymer Journal*, vol. 3, no. 5, pp. 600-610, 2011. DOI: https://doi.org/10.1295/polymj.3.600

[28] K. Matsushige, T. Takemura, " Melting point of oriented poly(vinylidene fluoride) form-i crystal under tensile stress", Journal of Polymer Science Part B: Polymer Physics, vol. 18, no. 7, pp. 1665-1669, July 1980. DOI: https://doi.org/10.1002/pol.1980.180180718

[29] A. Lopes, P. Martins and S. Lanceros-Mendez, “Polímeros piezoelétricos : Caraterísticas , aplicações , perspetivas” in Gazeta de Física, vol. 37, no. 3, pp. 2–7 December 2014. [Online]. Available from: https://www.spf.pt/magazines/GFIS/115/pdf [Accessed: 29/01/2018].

[30] D. Esterly, Manufacturing of Poly(vinylidene fluoride) and Evaluation of its Mechanical Properties, MSc., Virginia Polytechnic Institute and State University, 2002.

[31] E. G. Fine, R. F. Valentini, R. Bellamkonda, and P. Aebischer, "Improved nerve regeneration through piezoelectric vinylidenefluoride-trifluoroethylene copolymer guidance channels" Biomaterials, vol. 12, no. 8, pp. 775–780, 1991. DOI: https://doi.org/10.1016/0142-9612(91)90029-A

[32] J. Nunes-Pereira et al., "Poly(vinylidene fluoride) and copolymers as porous membranes for tissue engineering applications" Polymer Testing, vol. 44, pp. 234–241, July 2015. DOI: https://doi.org/10.1016/j.polymertesting.2015.05.001

[33] D. M. Correia et al., "Strategies for the development of three dimensional scaffolds from piezoelectric poly(vinylidene fluoride)" Materials & Design, vol. 92, pp. 674–681, February 2016. DOI: https://doi.org/10.1016/j.matdes.2015.12.043

[34] J. B. Rubin, L. B. Davenhall, C. M. V. Taylor, L. D. Sivils and T. Pierce, " A comparison of chilled DI water/ozone and CO2-based supercritical fluids as replacements for photoresist-stripping solvents", 23rd International Electronics Manufacturing Technology Symposium, May, 1999. [Online]. Available from: http://citeseerx.ist.psu.edu/viewdoc/summary?doi=10.1.1.544.6811 [Accessed: 14/11/2018].

[35] G. Brunner, "Supercritical fluids: technology and application to food processing", Journal of Food Engineering, vol. 67, no. 1, pp. 21-33, 2005. DOI: https://doi.org/10.1016/j.jfoodeng.2004.05.060

[36] Y. W. Kho, D. S. Kalika, B. L. Knutson, "Precipitation of Nylon 6 membranes using compressed carbon dioxide", Polymer, vol. 42, no 14, pp. 6119–6127.

[37] A. G. Mikos *et al.*, "Preparation and characterization of poly(l-lactic acid) foams," *Polymer (Guildf).*, vol. 35, no. 5, pp. 1068–1077, March 1994. DOI: https://doi.org/10.1016/0032-3861(94)90953-9

[38] M. Temtem, T. Casimiro, A. Aguiar-Ricardo, "Solvent Power and depressurization rate effects in the formation of polysulfone membranes with CO_2-assisted phase inversion method", *Journal of Membrane Science*, vol. 283, Issues 1-2, pp. 244-252, October 2006. DOI: https://doi.org/10.1016/j.memsci.2006.06.037

[39] M. Temtem, T. Casimiro, A. Aguiar-Ricardo, "Preparation of membranes with polysulfone/polycaprolactone blends using a high pressure cell specially designed for a CO_2-assisted phase inversion", *Journal of Supercritical Fluids*, vol. 43, Issue 3, pp. 542-548, January 2008. DOI: https://doi.org/10.1016/j.supflu.2007.07.012

[40] D.F. Williams, "Definitions in biomaterials", Journal of Polymer Science: Polymer Letters Edition, vol 26, issue 9, pp. 414, Amsterdam, 1988. DOI: 10.1002/pol.1988.140260910

[41] A. Oyane, H. K. Kim, T. Furuya, T. Kokubo, T. Miyazaki, T. Nakamura, "Preparation and assessment of revised simulated body fluids", Journal of Biomedical Material Research, vol 65A, no. 2, pp. 188–195, 2003. DOI: https://doi.org/10.1002/jbm.a.10482

[42] Organisation Internationale de Normalisation, "ISO 10993-5:2009: Biological evaluation of medical devices - Part 5: Tests for in vitro cytotoxicity", [Online]. Available: https://www.iso.org/standard/36406.html [Accessed: 16- Jan- 2019].

[43] A. L. Ahmad, N. Ideris, B. S. Ooi, S. C. Low and A. Ismail, "Influence of Polymer Concentration on PVDF Membrane Fabrication for Immunoassay Analysis", Journal of Applied Sciences, vol. 14, Issue 12, pp. 1299–1303, 2014. DOI: https://scialert.net/abstract/?doi=jas.2014.1299.1303

[44] I. Y. Abdullah, M. H. H. Jumali, M. Yahaya, H. M. Shanshool, "Facile Formation of β Poly (vinylidene fluoride) Films using the Short Time Annealing Process", Advances in Environmental Biology, vol. 9, no. 20, pp. 20–27, 2015. ISSN-1995-0756

[45] F. Mokhtari, M. Lafiti and M. Shamshirsaz, "Electrospinning/electrospray of polyvinylidene fluoride (PVDF): piezoelectric nanofibers", The Journal of The Textile Institute, vol. 107, no. 8, pp. 1037–1055, 2016. DOI: https://doi.org/10.1080/00405000.2015.1083300

[46] Damaraju, S. M., Wu, S., Jaffe, M., & Arinzeh, T. L. (2013). Structural changes in PVDF fibers due to electrospinning and its effect on biological function, 45007. DOI: https://doi.org/10.1088/1748-6041/8/4/045007

[47] S. M. Damaraju, S. Wu, M. Jaffe and T. L. Arinzeh, "Structural changes in PVDF fibers due to electrospinning and its effect on biological function", Biomedical Materials, vol. 8, no. 4, pp. 1-11, June 2013. DOI: https://doi.org/10.1080/00405000.2015.1083300

[48] K. Tanaka-Kamioka, H. Kamioka, H. Ris and S. Lim, "Osteocyte Shape Is Dependent on Actin Filaments and Osteocyte Processes Are Unique Actin-Rich Projections", Journal of Bone and Mineral Research, vol. 13, Issue. 10, pp. 1555-1568, October 1998. DOI: https://doi.org/10.1359/jbmr.1998.13.10.1555

6

Annexes

1 – EDS report for the 24h thermal treated sample

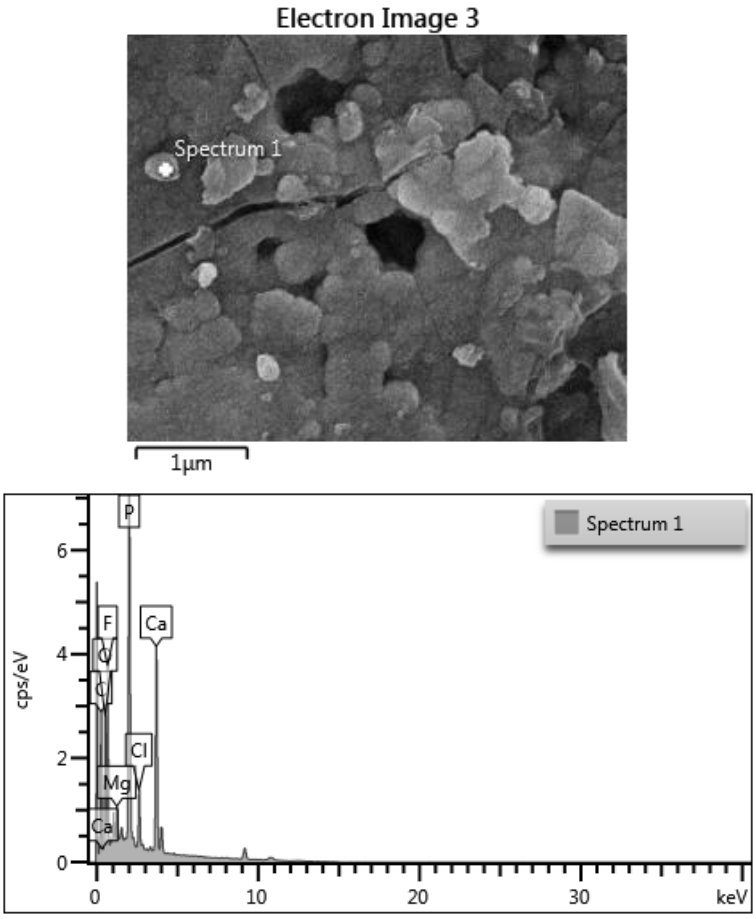

Element	Line Type	Apparent []	k Ratio	Wt%	Wt% Sigma	Atomic %	Standard Label
C	K series	0.17	0.0017	25.90	0.62	40.34	C Vit
O	K series	0.34	0.0011	17.03	0.45	19.91	SiO_2
F	K series	0.82	0.0016	20.24	0.41	19.93	CaF_2
Mg	K series	0.04	0.0002	1.55	0.09	1.19	MgO
P	K series	0.66	0.0037	14.31	0.23	8.64	GaP
Cl	K series	0.10	0.0008	3.27	0.11	1.72	NaCl
Ca	K series	0.55	0.0048	17.72	0.25	8.27	Wollastonite
Total:				100.00		100.00	

$$\frac{Ca}{P} = 0.94$$

2 – EDS report for the 5-day thermal treated sample

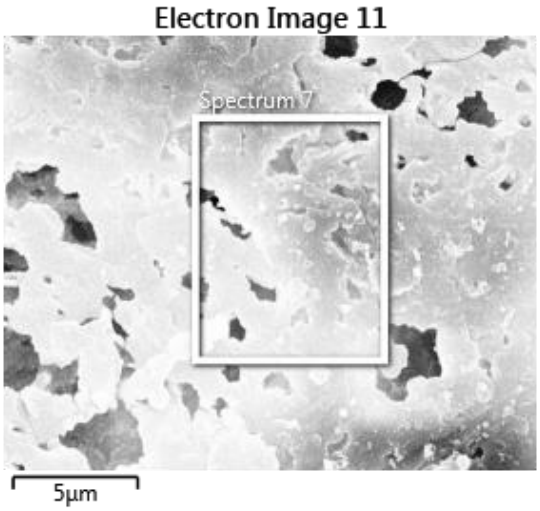

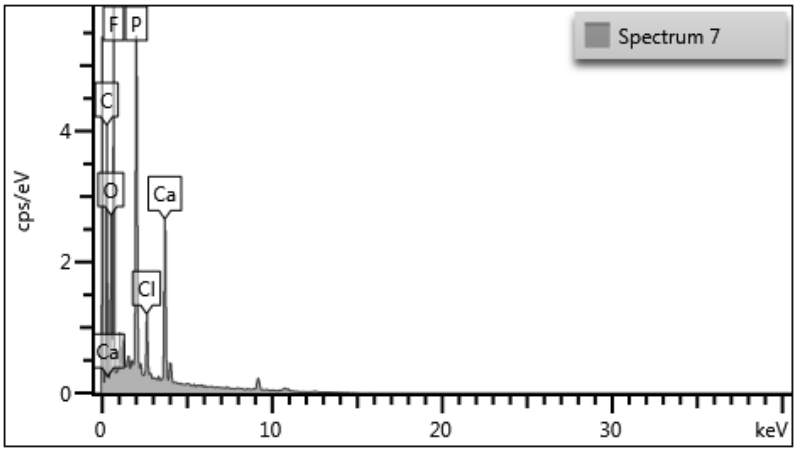

Element	Line Type	Apparent []	k Ratio	Wt%	Wt% Sigma	Atomic %	Standard
C	K series	0.26	0.0026	33.01	0.73	47.19	C Vit
O	K series	0.32	0.0010	13.93	0.53	14.94	SiO_2
F	K series	1.35	0.0026	28.68	0.55	25.92	CaF_2
P	K series	0.50	0.0028	10.75	0.25	5.96	GaP
Cl	K series	0.08	0.0007	2.74	0.13	1.33	NaCl
Ca	K series	0.34	0.0030	10.88	0.23	4.66	Wollastonite
Total:				100.00		100.00	

$$\frac{Ca}{P} = 0.78$$

3 – EDS report for the 24h positively polarized sample

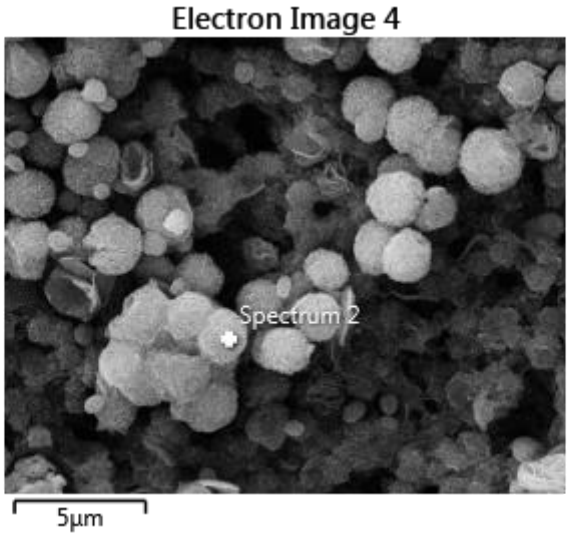

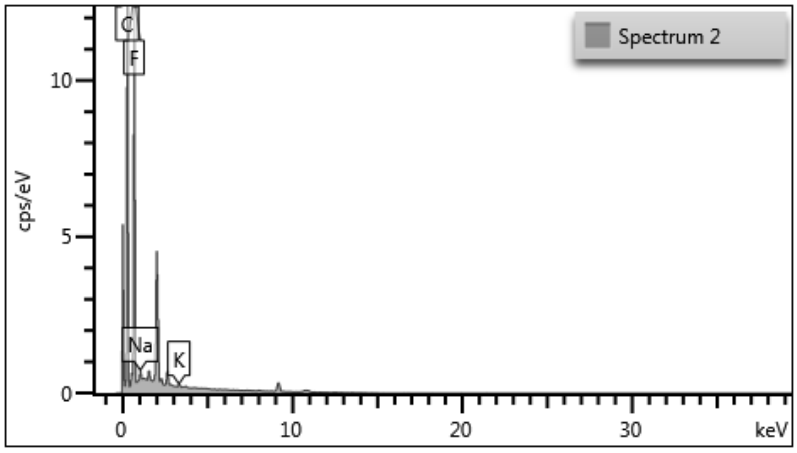

Element	Line Type	Apparent []	k Ratio	Wt%	Wt% Sigma	Atomic %	Standard Label
C	K series	0.81	0.0081	52.26	0.49	63.58	C Vit
F	K series	3.14	0.0061	46.41	0.48	35.69	CaF_2
Na	K series	0.03	0.0001	0.90	0.11	0.57	Albite
K	K series	0.01	0.0001	0.42	0.07	0.16	KBr
Total:				100.00		100.00	

4 – EDS report for the 5-day positively polarized sample

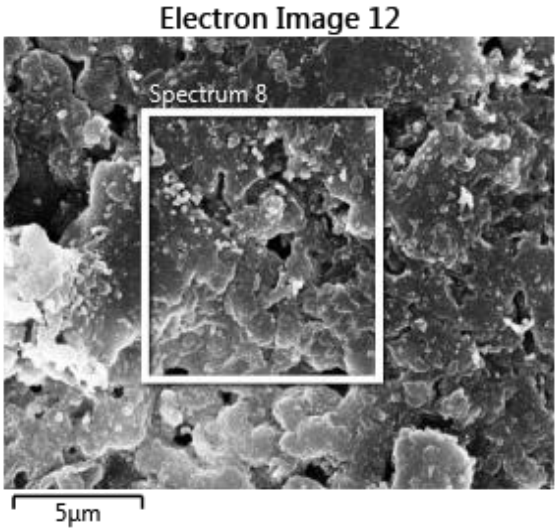

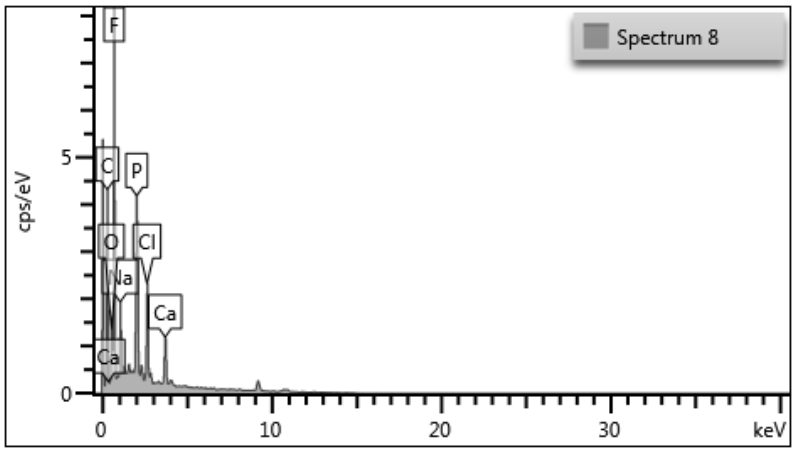

Element	Line Type	Apparent []	k Ratio	Wt%	Wt% Sigma	Atomic %	Standard Label
C	K series	0.28	0.0027	39.45	0.76	54.17	C Vit
O	K series	0.12	0.0004	5.17	0.42	5.33	SiO_2
F	K series	1.95	0.0038	33.33	0.56	28.94	CaF_2
Na	K series	0.14	0.0005	4.07	0.18	2.92	Albite
P	K series	0.35	0.0019	7.52	0.22	4.00	GaP
Cl	K series	0.18	0.0016	6.06	0.18	2.82	NaCl
Ca	K series	0.14	0.0012	4.4	0.16	1.81	Wollastonite
Total:				100.00		100.00	

$$\frac{Ca}{P} = 0{,}46$$

5 – EDS report for the 24h negatively polarized sample

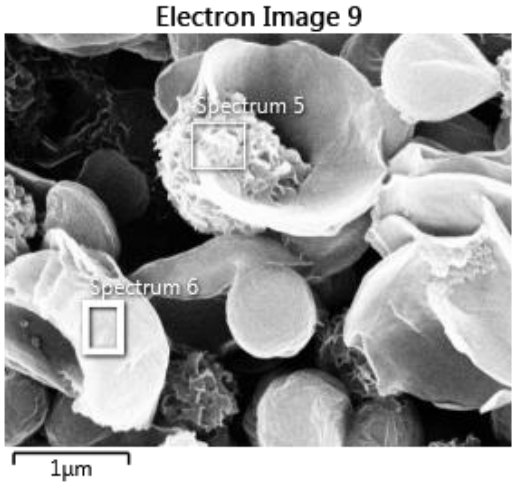

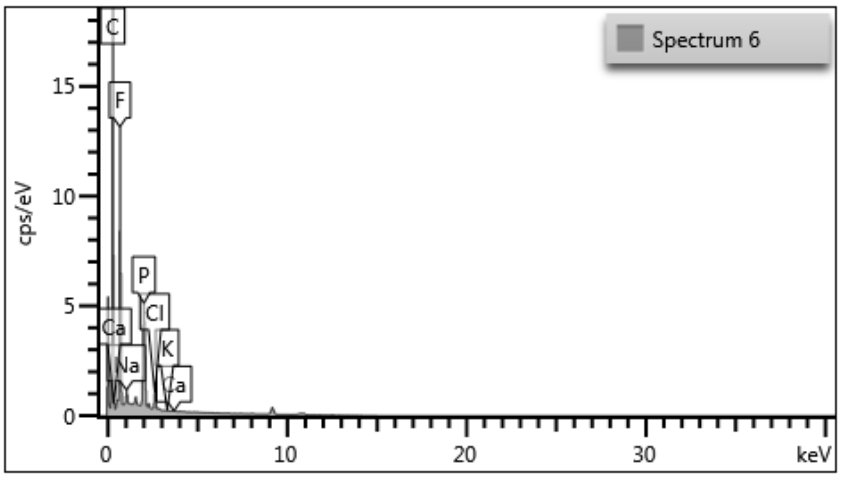

Element	Line Type	Apparent []	k Ratio	Wt%	Wt% Sigma	Atomic %	Standard Label
C	K series	1.17	0.0117	60.41	0.40	72.26	C Vit
F	K series	3.19	0.0062	31.91	0.35	24.13	CaF_2
Na	K series	0.05	0.0002	0.93	0.07	0.58	Albite
P	K series	0.39	0.0021	5.17	0.11	2.40	GaP
Cl	K series	0.07	0.0006	1.43	0.06	0.58	NaCl
K	K series	0.00	0.0000	0.08	0.04	0.03	KBr
Ca	K series	0.00	0.0000	0.07	0.04	0.03	Wollastonite
Total:				100.00		100.00	

$$\frac{Ca}{P} = 0{,}01$$

6 – EDS report for the 5-day negatively polarized sample

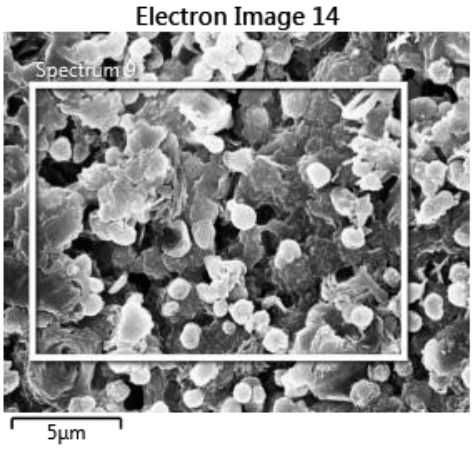

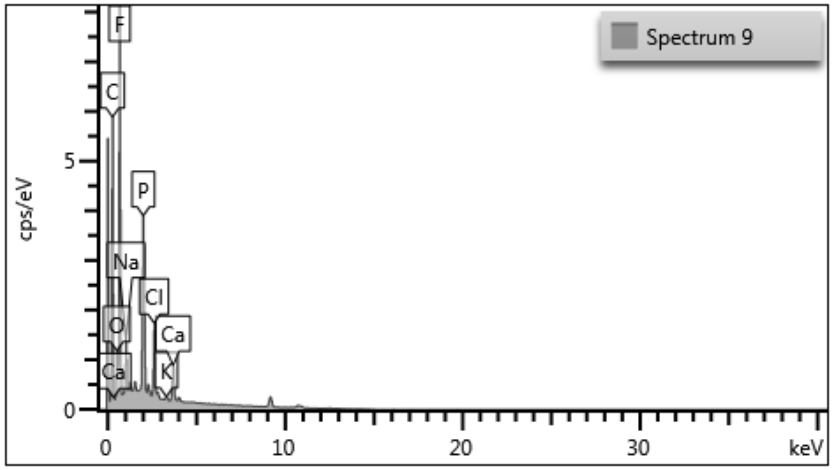

Element	Line Type	Apparent []	k Ratio	Wt%	Wt% Sigma	Atomic %	Standard Label
C	K series	0.34	0.0034	44.27	0.75	58.65	C Vit
O	K series	0.09	0.0003	4.03	0.32	4.01	SiO_2
F	K series	1.94	0.0038	33.90	0.53	28.39	CaF_2
Na	K series	0.09	0.0003	2.78	0.13	1.93	Albite
P	K series	0.32	0.0017	7.07	0.18	3.63	GaP
Cl	K series	0.13	0.0011	4.48	0.13	2.01	NaCl
K	K series	0.01	0.0000	0.31	0.07	0.13	KBr
Ca	K series	0.09	0.0008	3.17	0.11	1.26	Wollastonite
Total:				100.00		100.00	

$$\frac{Ca}{P} = 0{,}35$$